

1 We really appreciate and thank the reviewers for the comments and corrections. We are
2 in agreement with almost all the suggestions and thus, they have been taken into account in the
3 revised version. Reviewer's comments (in bold) and our answers below. After that, manuscript
4 with tracked changes is provided. It should be noted that the original structure of the manuscript
5 submitted to the open discussion process has been modified due that *Age model development*
6 Section (old Section 4) is shown now in the Supplementary Information (Section 1).
7

8 **RESPONSE TO COMMENTS OF ANONYMOUS REFEREE #1**

9
10
11
12
13 **1. About sample heterogeneity and representativity of reconstructed signals the E-P**
14 **balance was estimated by correcting temperature effect on *G. bulloides* $\delta^{18}\text{O}$ with Mg/Ca-**
15 **SST obtained on the same organism. However, the samples for Mg/Ca and $\delta^{18}\text{O}$**
16 **measurements were separately prepared although it could be possible to crush,**
17 **homogenise and mechanically clean test fragments before splitting for Mg/Ca and $\delta^{18}\text{O}$**
18 **analysis. Taking into account the small variability of signals, what would be the size of**
19 **uncertainty related to sample heterogeneity?**
20

21 -Specimens for Mg/Ca and $\delta^{18}\text{O}$ measurements were picked together from a very
22 restrictive size range (250-355 microns) but then crushed and cleaned separately, this is now
23 better described in the Section 3.5 of the manuscript. Certainly, both Mg/Ca and $\delta^{18}\text{O}$ values can
24 be size-dependent (Elderfield et al., 2002) but this effect can be minimized when the picking is
25 performed within a narrow size range. Reported $\delta^{18}\text{O}$ and Mg/Ca data in *G. bulloides* within the
26 size fraction of 250-300 microns and 300-355 microns show a range of variability of 0.13‰ and
27 0.31 mmol mol⁻¹ respectively. This could potentially be the range of expected sample
28 heterogeneity for the analysed samples. Nevertheless, the fact that the picking process for both
29 measurements was performed together, within a narrow size fraction, and the samples split later
30 in two sub-samples, can minimize the sample heterogeneity derived from selective picking of
31 different size fractions during independent picking processes.
32

33
34 **Since core MR3.1 was splitted into MR3.1A and MR3.1B, and the splitted samples were**
35 **separately analyzed, scatter plot of *G. bulloides* Mg/Ca, $\delta^{18}\text{O}_c$ and calculated $\delta^{18}\text{O}_{sw}$**
36 **obtained for MR3.1A and MR3.1B will allow evaluating such internal variability.**
37

38 -This is an interesting suggestion, we have performed this comparison and the obtained
39 average of the suggested internal variability has been ± 0.09 mmol mol⁻¹ in the Mg/Ca records
40 (Figure A1), which is equivalent to approximately $< 0.15^\circ\text{C}$ and very close to those reported by
41 Elderfield et al., (2002). In reference to $\delta^{18}\text{O}_c$ records and the calculated $\delta^{18}\text{O}_{sw}$, averages of the
42 obtained differences have been ± 0.05 VPDB‰ and ± 0.10 SMOW‰, respectively.
43

44
45 **In relation to the above-mentioned point, it is not clear how core MR3.1A Mg/Ca data**
46 **obtained with the reductive step were converted into SST values. This point should be**
47 **added to the text, and again the scatter plot will provide information on cleaning effect**
48 **and sample heterogeneity.**
49

50 -The Mg/Ca decrease of 23% by the reductive step in core MR3.1A was estimated by
51 comparison with the obtained Mg/Ca values in MR3.1B no cleaned with the reductive step
52 (Figure A1). Therefore, Mg/Ca values in MR3.1A were increased by 23% and then, SSTs were
53 calculated following the same calibration than the other cores. This explanation has been added
54 in Section 3.5 of the manuscript.

55
56
57
58
59
60
61
62
63
64
65
66
67
68
69
70
71
72
73
74
75
76
77
78
79
80
81
82
83
84
85
86
87
88
89
90
91
92
93
94
95
96
97
98
99
100
101
102
103
104
105
106
107
108
109
110
111

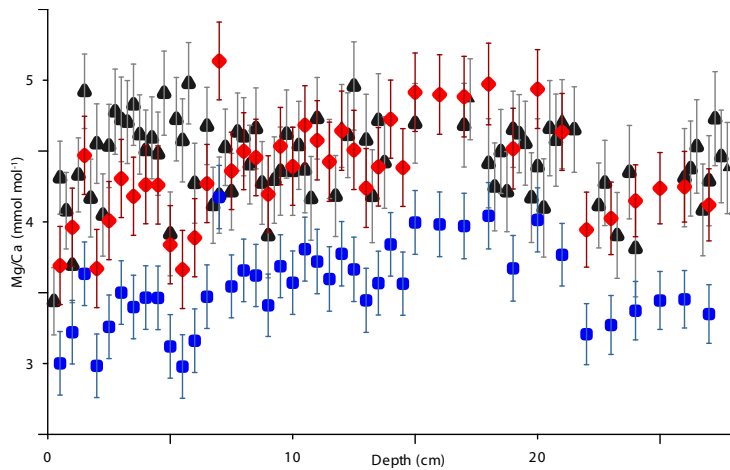


Fig. A1: Comparison of Mg/Ca records derived from the two halves of the same core MR3: MR3.1B (black triangles), and MR3.1A (blue squares) and MR3.1A after the correction of 23% (red rhombus). Vertical bars represent Mg/Ca uncertainties in the reproducibility of each analysis.

Besides, the Mg/Ca decrease of 23% by the reductive step is quite large compared to the general offset of 8 to 10% (Barker et al., 2003; Yu et al., 2007). Indeed, Pena et al. (2005) reported a larger offset but the studied samples contain Mn carbonates with high Mg. What would be possible reasons for this strong cleaning effect observed for the Minorca samples?

-There is not any exhaustive study about the effect of the reductive step in different foraminifera species. Yu et al., (2007) worked with benthic foraminifera and they could potentially be more resistant to dissolution. Barker et al (2003) worked with different planktonic species reporting an average Mg/Ca lowering of about 15%. Fig. 3 in Barker et al., (2003) show that significant differences exist between the considered species but for this part of the study, Barker et al. did not include *G. bulloides*. It could be the case that a species highly porous such as *G. bulloides* would be more sensitive to dissolution. Comments on this have been implemented in Section 3.5 of the manuscript.

Another way to evaluate the representativity of signals is to compare with Mg/Ca-SST and $\delta^{18}\text{O}$ of *G. bulloides*, estimated $\delta^{18}\text{O}_{\text{sw}}$ and U^{K}_{37} -SST already obtained for the Minorca site over the last 2000 years (Moreno et al., 2012).

These comparisons will allow estimating the size of significant variability. The authors may add the related uncertainty of reconstructed signals to the stack records. This will help distinguishing robust variability from internal noise and reinforce the interpretation developed in discussion section.

-We do not think that the proposed comparison with Moreno et al., (2012) data could necessarily provide information on the representativity of the signal. The data published by Moreno et al., (2012) in the Menorca Rise are part of the data set already used in this study. Both Mg/Ca and U^{K}_{37} records from that study are incorporated in this manuscript (MIN 1 and

112 2) but chronologies have been improved according to the description in Section 1 of
113 Supplementary Information and SST calibrations have been changed to include data from
114 Mediterranean core tops (see Section 4.1). Consequently, comparison with Moreno et al.,
115 (2012) can not provide any further information. We are not sure if it is proposed in here to use
116 the actual comparison between different proxies Mg/Ca and U^{K}_{37} , to assess the representativity
117 of the record. As it is already argued in our manuscript (Sections 4.1 and 4.5) we interpret that
118 *G. bulloides*-Mg/Ca-SST are representative of spring season, consistent with the reported period
119 of *G. bulloides* bloom in the region and with the comparison of our SST reconstructions with a
120 oceanographic data compilation of the region (MEDAR GROUP, 2002). In contrast, U^{K}_{37} is
121 interpreted to reflect a more annual average biased towards the colder season since
122 coccolithophoral productivity in summer is extremely low (see discussion in section 4.5). For this
123 reason these two records do not represent the same climatic signal and cannot be used to assess
124 the representativity of individual proxies.

125
126 **2. About the chronological constrains using geochemical data. The peaks of Mn XRF**
127 **intensity of bulk sediments and of foraminiferal Mn/Ca (not cleaned with a reductive step)**
128 **are expected to be almost synchronous because they both reflect redox state of pore water.**
129 **In contrast, reductively cleaned planktonic foraminiferal Mn/Ca values were used as an**
130 **indicator of seawater Mn concentration in water column where planktonic foraminifer**
131 **calcified (Klinkhammer et al., 2009). Since foraminiferal Mn contents of core MR3.1A**
132 **were obtained with a reductive cleaning, it is not obvious whether the synchronous peaks**
133 **with Mn XRF intensity of bulk sediments are expected (Figure 6, now Figure S5 in**
134 **Supplementary Information).**
135 **It will be interesting to present the foraminiferal Mn concentration as Mn/Ca ratio (Fig.**
136 **6, figure caption and the text) since the value of this ratio would allow distinguishing pore**
137 **water or seawater origin Mn.**
138

139 -This is a good observation, since Mn concentration in foraminifera tests after the
140 reductive cleaning not necessarily should reflect pore water conditions. This is only the case of
141 record MR3.1A. It has to be noted that the selected tie points in this case have mostly been
142 defined in base to its pair record, MR3.1B, where reductive cleaning was not applied and
143 structures are very similar to those of core MR3.2 measured by XRF scanner. For that reason,
144 although some questions can arise on the source of the Mn signal in *G. bulloides* the pair record
145 provides a solid evidence to correlate this core to others.

146
147
148 **Another concern about the chronological constrains with geochemical data is difference of**
149 **data resolution. The tie points shown in Figure 5 (Mg/Ca-SST) and Figure 6 (Mn) seem to**
150 **be affected by temporal resolution of records (now Figure S4 and S5 in Supplementary**
151 **Information). For instance MR3.1B foraminiferal Mn and bulk sediment XRF Mn peaks**
152 **are not totally synchronous because of different resolution of the records (Fig. 6b). Since**
153 **the initial age constrain was established by Bayesian models, I believe that the authors**
154 **created the coherent age model. However, assessment of age uncertainty will be useful to**
155 **avoid over-interpretation in the future studies.**
156

157 -This is also a good observation, chronological error for those cores based on
158 stratigraphical tools, will rely in the sedimentation rates and sampling resolution. This is now
159 took in account and indicated in a new table prepared for the Supplementary Information (Table
160 S4).

161
162
163
164
165
166

Minor or specific comments of Anonymous Referee #1

Page 14, lines 336-340, about the biostratigraphical constrain. It is necessary to add a short explanation why the peak of *G. quadrilobatus* and *G. truncatulinoides* (left coiling) are expected to be synchronous between Minorca site and southern Tyrrhenian Sea.

-Short explanations about this issue have been included in the Supplementary Information (Section 1.2) and are commented in more detail here:

It is well known that in the Mediterranean area, the planktonic foraminiferal distributions (First and Last Occurrence) as well as the acme (short intervals of abundance increasing) and paracme (short intervals of abundance decreasing) intervals are isochronous. This is well known for the last 23 Myr (i.e., for the Miocene: Di Stefano et al., 2015; Iaccarino et al., 2011; for the Calabrian: Maiorano et al., 2010; for the last 370ka: Piva et al., 2008; for the last 30kyr: Sprovieri et al., 2003; Melki et al., 2009; Budillon et al., 2009; Rouis-Zargouni et al., 2010; for the last millennia: Sprovieri et al., 2003; Lirer et al., 2013; Di Bella et al., 2014).

In Piva et al., (2008) it is evident that for the last 370 kyr, comparing the Adriatic and the Ionian seas, the abundance peaks of *Globigerinoides sacculifer* (corresponding to the *G. quadrilobatus* gr. in our manuscript) fall in the same short time intervals. The same framework is recorded for the *Globorotalia truncatulinoides*. It means that these short abundance intervals represent important events for high-resolution correlation between the Mediterranean.

Concerning the acme interval of *Globigerinoides quadrilobatus*, Lirer et al., (2013) documented the comparison between Tyrrhenian Sea and Sicily channel. However, if we consider also Budillon et al., (2009) from Sardinia channel, this event is well documented also in the central-western Mediterranean. In addition, if we observe the distribution pattern of the leaving planktonic foraminifera reported in Pujol and Vergnaud-Grazzini (1995), it is also evident that *G. quadrilobatus* is present in the entire western Mediterranean (excluding the Gulf of Lion). It means that the environmental parameters for this species are present in the western Mediterranean.

Conversely, the abundance peak of *Globorotalia truncatulinoides* during the Maunder, is documented only in the Lirer et al., (2013), because it is very difficult to find a marine record with this time interval well preserved and with this high-resolution time constrain. However, as reported by Piva et al., (2008), the abundance peaks of *G. truncatulinoides* during the last 370 kyr are well documented between Adriatic and Ionian seas. However, for the *G. truncatulinoides*, it is also important to see the geographical distribution map of this species reported in Thunell (1978) for the Recent Planktonic Foraminifera in Surface Sediments of the Mediterranean Sea. It is evident that this species is present from Balearic Islands to Sicily channel. The same information is also documented if we observe the distribution pattern of the leaving *G. truncatulinoides* foraminifera, reported in Pujol and Vergnaud-Grazzini (1995), where this species is present in the entire western Mediterranean.

Finally, Geraga et al. (2005) show the possibility to identify the different abundance peaks, documented in several planktonic foraminiferal species by Pérez-Folgado et al. (2003) in the Alboran Sea, also in the Aegean Sea.

Page 33, lines 795-797 and Figure 13 (now Figure 8), about the relationship between $\delta^{18}\text{O}_{\text{sw}}$ and NAO. The proposed correlation is not clear with Figure 13. If it is statistically significant, modification of $\delta^{18}\text{O}_{\text{sw}}$ stack scale may be necessary.

-The obtained correlations between $\delta^{18}\text{O}_{\text{sw}}$ and NAO are not statistically significant, and we did not want to claim a high correlation, but we wanted to express that for the last 1000 yr a more coherent pattern of low $\delta^{18}\text{O}_{\text{sw}}$ and negative NAO exists. Welch's test results indicate that the null hypothesis (difference between means is 0) cannot be discarded for both proxies, at 5% error level ($t_{\text{observed}} = -0.109 < t_{\text{critical}} = 1.960$). Although, as the text mentions, the connection

222 between NAO and $\delta^{18}\text{O}_{\text{sw}}$ looks rather complex, other factors could have acted and as it is
223 discussed, it does not seem that all NAO- or NAO+ conditions have identical response in the
224 Western Mediterranean conditions. This part of the text has now been rephrased to avoid
225 confusion in this part. The proposed change in scales have been done to improve the
226 comparison.

227
228

229 **Figure 7 (now Figure 2). The sample with the highest Mg/Ca value is offset from the**
230 **general trend. Which core indicates this data point?**

231
232

233 -The highest Mg/Ca value corresponded to core KTB-34. This sample presented a
234 significant off set from the rest but any evidence, such as anomalous values of $\delta^{18}\text{O}_{\text{sw}}$ or other
235 trace metal ratios (Mn/Ca or Al/Ca) existed to reject it and we decided that it was more honest
236 to include it in the data set. However, in order to minimize error of temperature estimates based
237 on our *G. bulloides* calibration for the Western Mediterranean and to improve confidence limits
238 of our equation, finally this core has not been taken into account in the new calibration now
239 proposed.

240

241 **Table 1. Indicate that Mg/Ca and $\delta^{18}\text{O}_c$ values are obtained for “*G. bulloides*” cleaned**
242 **without a reductive step. The unit for $\delta^{18}\text{O}$ “VPDB‰” should be added. If age control of**
243 **each core-top is available, it is useful to show it. If not, at least indicate corer types in the**
244 **text.**

245
246

247 -These suggestions have been incorporated on the Table S4 (Supplementary
248 Information). At the end of section 3.1 is indicated that cores used in calibration are multicores.
249 And also in section 4.1 more information about them has been incorporated: their core-tops can
250 be considered as representative of near or present conditions (Masqué et al., 2003; Cacho et al.,
2006).

251
252

253

254 **RESPONSE TO COMMENTS OF ANONYMOUS REFEREE #2**

255
256

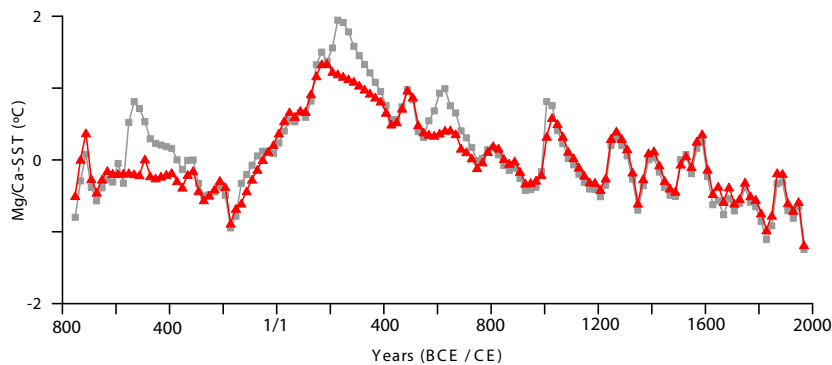
257 **p. 5449 there are several potential analytical issues here. In particular, correlations**
258 **between Mg/Ca and Al need to be carefully assessed for significance (i.e., P value) rather**
259 **than just rejected based on the R value. If the correlations are significant, then that**
260 **indicates that there is some detrital contribution to Mg/Ca (Barker et al, 2003; Lea et al,**
261 **2005)**

262

263 -We have re-examined the correlations of Mg/Ca with Al and also Mn and we recognise
264 that we did probably underestimate the potential interference of some contamination phases
265 since ratios measured in cores MIN1, MR3.1B and MR3.3 presented significant correlations.
266 In order to minimize the risk of Mg/Ca-SST overestimations due to detrital/diagenetic
267 contamination, a rejection criteria was established, discarding those samples presenting Mn/Ca
268 ratios above $0.5 \text{ mmol mol}^{-1}$ in core MR3.1B although in cores MIN1 and MR3.3 the
269 threshold was relaxed to those ratios above $>1 \text{ mmol mol}^{-1}$. The reason for this criteria
270 relaxation was the absence of significant correlation ($r < 0.28$, $p\text{-value}=0.06$) after its
271 application. We considered that this was a good compromise to minimize contamination risks
272 without a significant lost of sample resolution. In the case of Al/Ca ratios, after the removal of
273 the two highest Mg/Ca values in core MR3.1B and those that more contributed to the
274 significance in core MIN1 (9 values), obtained correlations were not significant ($r < 0.29$, $p\text{-}$
275 $\text{value}=0.06$). This information has been incorporated in the manuscript (Section 3.5).

276

277 Consequently, the Mg/Ca-SST anomaly stack is now different, as can be observed in Figure A2,
 278 but does not introduce significant changes in the main patterns and structures and therefore,
 279 neither in the discussion already published during the open Discussion process (Figure A2).
 280 Some minor modifications have been included in the final text (i.e. quantification of SST
 281 changes) and the figures but they not have involved significant variations.
 282



283 **Fig. A2:** Comparison of Mg/Ca-SST anomaly stacks published during Open Discussion (grey squares)
 284 and after removing with potential contamination problems on trace element data treatment (red triangles).
 285
 286
 287

288 ***p. 5549 the choice of the Shackleton 1974 paleotemp equation is an odd one,**
 289 **because this equation was developed for benthic ff. Some bulloides-specific equations such**
 290 **as Bemis et al., 1998 have been developed. The authors should try these or others, as**
 291 **appropriate, and justify their final choice.**
 292
 293

294 -We do not consider that this is an odd choice since it is the most used equation in
 295 similar estimations, nevertheless, referee is very right pointing out that it was developed in base
 296 to benthic foraminifera but, it actually confirmed the relation-ship with inorganic calcite
 297 precipitation (Epstein et al., 1953) suggesting very little or null biologic effect in this case.
 298 Nevertheless we agree with the referee that more recent studies carried on cultured planktonic
 299 species have shown that, although the slope is rather constant, the intercepts of the equation
 300 may present differences to some degree depending on the species and also on its size range
 301 (Bemis et al., 1998). Following this referee suggestion, we have recalculate the $\delta^{18}\text{O}_{\text{sw}}$ values
 302 from the core top samples (Table A1) using the regression equations published for culture-
 303 derived *Globigerina bulloides* (11-chambered shell equation in Bemis et al., 1998) and those
 304 resulting from plankton-town *G. bulloides* collection (Mullitza et al., 2003). The obtained $\delta^{18}\text{O}_{\text{sw}}$
 305 values (2.1-1.5 SMOW‰) are higher than those (~1.2 SMOW‰) published by (Pierre 1999)
 306 based in water measurements from the central-western Mediterranean Sea. In contrast, those
 307 values previously estimated with the empirical Shackleton (1974) paleotemperature equation
 308 provide $\delta^{18}\text{O}_{\text{sw}}$ values of 1.0-1.2 SMOW‰ and consequently closer to the present day water
 309 values. In base to this result we have decided to stay better with our original estimate. Several
 310 factors may account for this different results but in front of the absence of specific experiments
 311 using Mediterranean species let us to consider that the more conservative approach using the
 312 general equation is probably the one more appropriate in this case. A comment on this has been
 313 added in Section 3.5.
 314
 315

316 **Table A1:** $\delta^{18}\text{O}_{\text{sw}}$ calculated according to different paleotemperature equations for core tops from Balears
 317 (time spanned ~last 50 years).

318

Core	Depth (cm)	$\delta^{18}\text{O}_c$ (VPDB‰)	Mg/Ca-SST (°C)	$\delta^{18}\text{O}_{\text{sw}}$ (SMOW‰) Shackleton, 1964	$\delta^{18}\text{O}_{\text{sw}}$ (SMOW‰) Bemis et al., 1998	$\delta^{18}\text{O}_{\text{sw}}$ (SMOW‰) Mulitza et al., 2003
MIN1	1	1.2	14.9	1.0	1.9	1.5
	1.5	1.1	16.2	1.2	2.1	1.7
MIN2	0.5	1.1	15.3	1.0	1.9	1.5
	1	1.1	15.5	1.1	2.0	1.6
MR3.1B	0.25	1.3	14.9	1.1	2.0	1.6

319

320

321

322

323

324

325

326

327

328

329

330

331

332

333

334

335

336

337

338

339

340

341

342

343

344

345

346

347

348

349

350

351

352

353

354

355

356

p. 5454-55 The alignment of the different cores via both Mg/Ca and Mn appears somewhat arbitrary; e.g., the peaks in Fig. 5-6 (now Fig. S4-S5 in Supplementary Information) could be aligned in a number of different ways. I understand that the authors are attempting to develop the best overall chronology for their records, but some added discussion about uncertainties in this context would be welcome. For example, how large is the effect on the final stacks of the proposed alignments?

-We agree in that alignments could be regarded to some extent arbitrary but, this is the reason why a special care has been done in performing the Bayesian age models to make sure that any alignment was performed within the uncertainty range of the statistical models. In this way we have always kept an objective criterion limiting our arbitrariness selecting structures to align. It has to be kept in mind that all cores have some absolute age indicator (^{14}C , biostratigraphy, Pb or Cs) that anchor the records in some points (within their uncertainties) limiting the potential arbitrariness in the alignments. There is only one exception to this, core MR3.1B for which any absolute age indicator exists, but this section corresponds to the second half from core MR3.1A and thus little uncertainties in the alignment of these two sections exist. It also probably worth to mention that an independent proof for our alignments was the comparison of the alignment on the grain-size record of the same cores. This information was removed for this manuscript because it was already too dense of data and it is the matter of an independent manuscript. But the coherence of the independent grain-size records after the alignment base in independent records give to us an independent objective argument to be convinced about the coherent alignment choice.

Nevertheless, taking in consideration the referee doubts we have performed an exercise of producing a different stack taking only the records with the Bayesian age model and before performing any alignment between them (Figure A3). The major trends do not differ between the two stacks neither the age of the main structures, the main difference is the appearance of enhanced climate variability along the Medieval Climate Anomaly, but looking to the records that is not reflected by any of them and it results as an artefact of the lack of alignment of some of the minor structures, for this reason we believe that the proposed stacks are the best expression of the analysed records, they average a total of five records providing a record of the most robust trends and oscillations.

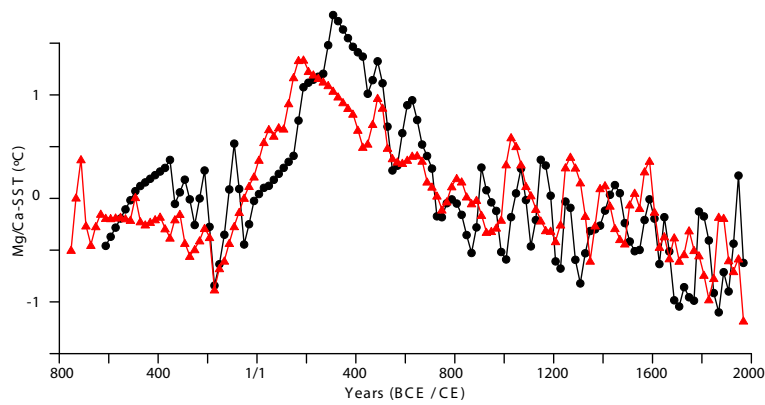


Fig. A3: Comparison of the Mg/Ca-SST anomaly stack with the final age-model (red triangles) with the stack taking only the records with the Bayesian age model (cores MIN1, MIN2 and MR3.3, which have absolute dates: ^{14}C and foraminiferal assemblage dates) and before performing any alignment between them (black circles).

p. 5457: the inference that *G. bulloides* represents Spring temperatures will be heavily influenced by the choice of calibration equations for O18 (see above). How would this inference change with a different calibration choice?

-When the *G. bulloides* specific equations (Bemis et al., 1998; Mulitza et al., 2003) are applied to estimate the isotopic temperatures of core top samples the values are about 0.6°C colder or 1°C warmer, respectively, than those obtained with the Shackleton's equation. Therefore, the resulting temperatures would still be within the present spring conditions but as is argued above we have some solid arguments to use the Shackleton's equation.

Along the same lines, how does the derived Mg/Ca calibration equation compare to previous ones? Does it agree within uncertainties?

-Several different temperature calibrations exist for *G. bulloides*-Mg/Ca ratios and in some cases they provide very different results when they are applied to our data (Table A3) and the differences are far above within the uncertainties, the larger difference is above 13°C. The manuscript does not pretend to make an analysis of the reason for this big calibration differences, obviously the approaches are very different and also the source region for the calibrated specimens. For that reason it makes a big difference the chosen calibration and we believe that the fact that, the used calibration is based on a previous published one reviewed after the addition of new data points covering the temperature range of our region, is a solid argument to support our choice.

p. 5461, difference between UK37' and Mg/Ca. This difference will also be sensitive to the calibration choice for *bulloides* O18. What do the uncertainties represent? Do the absolute values between the two temperature proxies differ according to a t-test?

-As it has been argued above, we believe that we have solid arguments to justify our choice for the *G. bulloides* $\delta^{18}\text{O}$ temperature equation and consequently, we are confident that this provides the values which better represent the local oceanographic conditions. As it is

396 described above, other choices of $\delta^{18}\text{O}$ equations applied in the calibration would provide
 397 slightly different values but this still won't account for the described differences between the
 398 U^{k}_{37} and Mg/Ca records, which differ in the intensity of the SST variability and short term
 399 oscillations.

400
 401 The SST uncertainties in the section 4.5 include analytical precision and reproducibility and
 402 also standard error derived from calibration. Alk-SST uncertainties in this section have been
 403 estimated to have a mean value of $\pm 1.1^\circ\text{C}$, taking into account the standard error of estimation
 404 (Conte et al., 2006). This is indicated now on the text.

405
 406 Regarding the proposed t-test: the Mg/Ca-SST and Alk-SST absolute values show a significant
 407 correlation ($r=0.5$; $p\text{-value}=0$) but results obtained by means of Welch's test indicate that the
 408 null hypothesis (means are equal) can be discarded at the 5% error level: $t_{\text{observed}}(12.446) > t_{\text{critical}}$
 409 (1.971) .

410
 411 **Table A3:** SST averages obtained from the 10 core top samples from the central-western Mediterranean
 412 Sea used in this study after applying the different published *G. bulloides* temperature calibrations and
 413 compared to the our study's calibration.
 414
 415

Mg/Ca = A exp (B * SST)	A	B	Core top SST average ($^\circ\text{C}$)
Mashiotta et al., (1999)	0.474	0.107	21.7
Lea et al., (1999)	0.53	0.1	19.4
Elderfield and Ganssen (2000)	0.56	0.1	18.6
Anand et al., (2003)	0.81	0.081	12.1
McConnell and Thunell (2005)	1.2	0.057	6.3
Cl�eroux et al., (2008)	0.78	0.082	12.6
Thornalley, Elderfield and McCave (2009)	0.794	0.1	15.1
Patton et al., (2011)	0.97	0.066	8.7
This study	0.7045	0.0939	15.3

416
 417
 418
 419 **p. 5462 (lines 20-23): (in reference to the Mg/Ca-SST and Uk37-SST comparison) it might**
 420 **also represent inadequacies in the data treatment and chronology. I suggest the authors**
 421 **consider multiple hypotheses to explain this difference.**

422
 423 -As described above, Mg/Ca data treatment has already been reviewed, following
 424 referee 2 suggestions, and the resulting data from this new treatment does not introduce any
 425 significant change in the discussed differences between the two different proxy stacks,
 426 supporting that these discrepancies are real and not artefacts from data treatment.
 427 However, after modification of our Mg/Ca-calibration equation, although average of both
 428 proxies are now more similar, the intensity of the Mg/Ca-SST variability and short term
 429 oscillations remains higher than Alk-SST.
 430

431
432 Regarding the potential artefact resulting from the use of inadequate chronologies, our
433 confidence in the chosen chronologies has already been argued above and their uncertainties
434 better expressed in Table S4 (Supplementary Information). But this factor can really be ignored
435 in the case of this proxy inter-comparison since it is based in exactly the same cores whose
436 chronology has been performed in this manuscript. Any change in the chronology would affect
437 in the same way both proxy records and consequently won't affect the discussed apparent anti-
438 phase in some of the structures.
439

440 **Section 6.1 (now Section 5.1): throughout this section, all temperature changes should be**
441 **given with attendant uncertainties, in part to make clear how significant the changes are.**
442

443 -The corresponding temperature uncertainties will be included in all the text.
444 Explanations about the type of uncertainty will be shown in the beginning of the corresponding
445 section or after the uncertainty.
446

447 **Section 6.2 (now Section 5.2): McGregor et al., 2015, NG, called on volcanism as the main**
448 **cause of the cooling trend of the last 1000 years. How does this forcing potentially**
449 **influence the**

450 **Med. records? Could it also play a role in driving centennial-scale variability?**
451

452 -No significant correlations have been obtained between Mg/Ca-SST or Alk-SST shown
453 in this study and volcanism in Northern Hemisphere (Gao et al., 2008), but the higher volcanism
454 in the last millennia could have acted as forcing in the general cooling trend observed in this
455 study, given the derived induction of a net negative radiative forcing as described in McGregor
456 et al. (2015). As is discussed in the text, several factors in addition to the summer insolation
457 should account to explain the centennial-scale variability of the records, some of them are
458 discussed and the potential impact of enhanced volcanism in the last millennia is now also been
459 introduced in the discussion (Section 5.2).
460

461
462
463
464
465
466
467
468
469
470
471
472
473
474
475
476
477
478
479
480
481
482
483
484
485

486
487
488
489
490
491
492
493
494
495
496
497
498
499
500
501
502
503
504
505
506
507
508
509
510
511
512
513
514
515
516
517
518
519
520
521
522
523
524
525
526
527
528
529
530
531
532
533
534
535
536
537
538
539
540

REFERENCES

(Related to response to comments of anonymous referee #1 and #2)

- Anand, P., Elderfield, H., and Conte, M. H.: Calibration of Mg/Ca thermometry in planktonic foraminifera from a sediment trap time series, *Paleoceanography*, 18, 1050, doi:10.1029/2002PA000846, 2003.
- Barker, S., Greaves, M., and Elderfield, H.: A study of cleaning procedures used for foraminiferal Mg/Ca paleothermometry, *Geochem. Geophys. Geosyst.*, 4, 9, doi:10.1029/2003GC000559, 2003.
- Bemis, B. E., Spero, H. J., Bijma, J. and Lea, D. W.: Reevaluation of the oxygen isotopic composition of planktonic foraminifera: Experimental results and revised paleotemperature equations, *Paleoceanography*, 13(2), 150–160, doi:10.1029/98PA00070, 1998.
- Budillon F., Lirer F., Iorio M., Macri P., Sagnotti L., Vallefucio M., Ferraro L., Innangi S., Sahabi M., Tonielli R.: Integrated stratigraphic reconstruction for the last 80 kyr in a deep sector of the Sardinia Channel (Western Mediterranean), *Deep. Sea. Res. Part II Top Stud. Oceanogr.*, 56, 725–737, 2009.
- Cacho, I., Shackleton, N., Elderfield, H., Sierro, F. J. and Grimalt, J. O.: Glacial rapid variability in deep-water temperature and $\delta^{18}\text{O}$ from the Western Mediterranean Sea, *Quat. Sci. Rev.*, 25, 3294–3311, doi:10.1016/j.quascirev.2006.10.004, 2006.
- Clérout, C., Cortijo, E., Anand, P., Labeyrie, L., Bassinot, F., Cailion, N., and Duplessy, J. C.: Mg/Ca and Sr/Ca ratios in planktonic foraminifera: proxies for upper water column temperature reconstruction, *Paleoceanography*, 23, PA3214, doi:10.1029/2007PA001505, 2008.
- Di Bella, L., Frezza, V., Bergamin, L., Carboni, M. G., Falese, F., Mortorelli, E., Tarragoni, C., and Chiocci, F. L.: Foraminiferal record and high-resolution seismic stratigraphy of the Late Holocene succession of the submerged Ombrone River delta (Northern Tyrrhenian Sea, Italy), *Quatern. Int.*, 328–329, 287–300, 2014.
- Di Stefano, A., Baldassini, N., Maniscalco, R., Speranza, F., Maffione, M., Cascella, A., Foresi, L.M.: New bio-magnetostratigraphic data on the Miocene Moria section (Northern Apennines, Italy): connections between the Mediterranean and the Atlantic Ocean. *Newsletters on Stratigraphy*, 48, 2, 135–152, doi: 10.1127/nos/2015/0057, 2015.
- Elderfield, H. and Ganssen, G.: Past temperature and $\delta^{18}\text{O}$ of surface ocean waters inferred from foraminiferal Mg/Ca ratios, *Nature*, 405, 442–445, 2000.
- Elderfield, H., Vaitravers, M. and Cooper, M.: The relationship between shell size and Mg/Ca, Sr/Ca, $\delta^{18}\text{O}$, and $\delta^{13}\text{C}$ of species of planktonic foraminifera, *Geochem. Geophys. Geosyst.*, 3, 8, doi:10.1029/2001GC000194, 2002.
- Epstein, S., Buchsbaum, R., Lowenstam, H. A., and Urey, H. C.: Revised carbonate-water isotopic temperature scale. *Bull. Geol. Soc. Am.*, 64, 1315–1326, 1953.
- Gao, C., Robock, A. and Ammann, C.: Volcanic forcing of climate over the past 1500 years: An improved ice core-based index for climate models, *J. Geophys. Res.*, 113, D23111, doi:10.1029/2008JD010239, 2008.
- Geraga, M., Tsaila-Monopolis, S., Ioakim, C., Papatheodorou, G., Ferentinos, G.: Short-term climate changes in the southern Aegean Sea over the last 48,000 years, *Paleogeogr. Paleoclimatol. Paleoecol.*, 220, 311–332, 2005.
- Iaccarino, S., Di Stefano, A., M. Foresi, L. M., Turco, E., Baldassini, N., Cascella, A., Da Prato, S., Ferraro, L., Gennari, R., Hilgen, F.J., Lirer, F., Maniscalco, R., Mazzei, R., Riforgiato, F., Russo, B., Sagnotti, L., Salvatorini, G., Speranza, F. and Verducci, M.: High-resolution integrated stratigraphy of the upper Burdigalian–lower Langhian in the Mediterranean: the Langhian historical stratotype and new candidate sections for defining its GSSP, *Stratigraphy*, 8, 199–215, 2011.
- Klinkhammer, G. P., Mix, A. C., and Haley, B. A.: Increased dissolved terrestrial input to the coastal ocean during the last deglaciation, *Geochem. Geophys. Geosyst.*, 10, Q03009, 2009.

541 Lea, D. W., Mashiotto, T. A., and Spero, H. J.: Controls on magnesium and strontium
542 uptake in planktonic foraminifera determined by live culturing, *Geochim. Cosmochim. Ac.*, 63,
543 2369–2379, 1999.

544 Lea, D. W., Pak, D. K., and Paradis, G.: Influence of volcanic shards on foraminiferal
545 Mg/Ca in a core from the Galápagos region, *Geochem. Geophys. Geosy.*, 6, 11,
546 doi:10.1029/2005GC000970, 2005.

547 Lirer, F., Sprovieri, M., Ferraro, L., Vallefucio, M., Capotondi, L., Cascella, A.,
548 Petrosino, P., Insinga, D. D., Pelosi, N., Tamburrino, S., and Lubritto, C.: Integrated
549 stratigraphy for the Late Quaternary in the eastern Tyrrhenian Sea, *Quatern. Int.*, 292, 71–85,
550 doi:10.1016/j.quaint.2012.08.2055, 2013.

551 Maiorano, P., Caspotondi, L., Ciaranfi, N., Girone, A., Petrosino, P.: Vrica-Crotone and
552 Montalbano Jonico Sections: A Potential Unit-Stratotype of the Calabrian Stage, *J. Int. Geosci.*,
553 33, 4, 2010.

554 Mashiotto, T. A., Lea, D. W., and Spero, H. J.: Glacial–interglacial changes in
555 Subantarctic sea surface temperature and $\delta^{18}\text{O}$ -water using foraminiferal Mg, *Earth Planet. Sc.*
556 *Lett.*, 170, 417–432, 1999.

557 Masqué, P., Fabres, J., Canals, M., Sanchez-Cabeza, J. A., Sanchez-Vidal, A., Cacho, I.,
558 Calafat, A. M., and Bruach, J. M.: Accumulation rates of major constituents of hemipelagic
559 sediments in the deep Alboran Sea: a centennial perspective of sedimentary dynamics, *Mar.*
560 *Geol.*, 193, 207–233, 2003.

561 McConnell, M. C. and Thunell, R. C.: Calibration of the planktonic foraminiferal
562 Mg/Ca paleothermometer: sediment trap results from the Guaymas Basin, Gulf of California,
563 *Paleoceanography*, 20, PA2016, doi:10.1029/2004PA001077, 2005.

564 McGregor, H. V., Evans, M. N., Goosse, H., Leduc, G., Martrat, B., Addison, J. A.,
565 Graham Mortyn, P., Oppo, D. W., Seidenkrantz, M.-S., Sicre, M.-A., Phipps, S. J., Selvaraj, K.,
566 Thirumalai, K., Filipsson, H. L. and Ersek, V.: Robust global ocean cooling trend for the pre-
567 industrial Common Era, *Nat Geosci.*, 8(9), 671–677, doi:10.1038/ngeo2510, 2015.

568 MEDAR GROUP, MEDATLAS/2002 European Project: Mediterranean and Black Sea
569 Database of Temperature Salinity and Bio-Chemical Parameters, Climatological Atlas, Institut
570 Français de Recherche pour L'Exploitation de la Mer (IFREMER), Edition/Instituto Nazionale
571 di Oceanografia e di Geofisica Sperimentale (OGS), 2002

572 Melki, T., Kallel, N., Jorissen, F. J., Guichard, F., Dennielou, B., Berné, S., Labeyrie, L.
573 and Fontugne, M.: Abrupt climate change, sea surface salinity and paleoproductivity in the
574 western Mediterranean Sea (Gulf of Lion) during the last 28 kyr, *Palaeogeogr. Palaeoclimatol.*
575 *Palaeoecol.*, 279, 1-2, 96–113, doi:10.1016/j.palaeo.2009.05.005, 2009.

576 Moreno, A., Pérez, A., Frigola, J., Nieto-Moreno, V., Rodrigo-Gámiz, M., Martrat, B.,
577 González-Sampériz, P., Morellón, M., Martín-Puertas, C., Pablo, J., Belmonte, Á., Sancho, C.,
578 Cacho, I., Herrera, G., Canals, M., Grimalt, J. O., Jiménez-Espejo, F., Martínez-Ruiz, F., Vegas-
579 Vilarrúbia, T., and Valero-Garcés, B. L.: The Medieval Climate Anomaly in the Iberian
580 Peninsula reconstructed from marine and lake records, *Quaternary Sci. Rev.*, 43, 16–32,
581 doi:10.1016/j.quascirev.2012.04.007, 2012.

582 Mulitza, S., Boltovskoy, D., Donner, B., Meggers, H., Paul, A. and Wefer, G.:
583 Temperature: $\delta^{18}\text{O}$ relationships of planktonic foraminifera collected from surface waters,
584 *Palaeogeogr. Palaeoclimatol. Palaeoecol.*, 202(1-2), 143–152, doi:10.1016/S0031-
585 0182(03)00633-3, 2003.

586 Patton, G. M., Martin, P. A., Voelker, A., and Salgueiro, E.: Multiproxy comparison of
587 oceanographic temperature during Heinrich Events in the eastern subtropical Atlantic, *Earth*
588 *Planet. Sc. Lett.*, 310, 45–58, doi:10.1016/j.epsl.2011.07.028, 2011.

589 Pena, L. D., Calvo, E., Cacho, I., Eggins, S., and Pelejero, C.: Identification and
590 removal of Mn-Mg-rich contaminant phases on foraminiferal tests: implications for Mg/Ca past
591 temperature reconstructions, *Geochem. Geophys. Geosy.*, 6, 9, doi:10.1029/2005GC000930,
592 2005.

593 Pérez-Folgado, M., Sierro, F. J., Flores, J. A., Cacho, I., Grimalt, J. O., Zahn, R. and
594 Shackleton, N.: Western Mediterranean planktonic foraminifera events and millennial climatic
595 variability during the last 70 kyr, *Mar. Micropaleontol.*, 48, 49–70, doi:10.1016/S0377-

596 8398(02)00160-3, 2003.
597 Pierre, C.: The oxygen and carbon isotope distribution in the Mediterranean water
598 masses, *Mar. Geol.*, 153, 41–55, 1999.
599 Piva, A., Asioli, A., Trincardi, F., Schneider, R. R., and Vigliotti, L.: Late-Holocene
600 climate variability in the Adriatic Sea (Central Mediterranean), *The Holocene*, 18, 153–167,
601 2008.
602 Pujol, C. and Vergnaud-Grazzini, C.: Distribution patterns of live planktic foraminifers
603 as related to regional hydrography and productive systems of the Mediterranean Sea, *Mar.*
604 *Micropaleontol.*, 25, 187–217, 1995.
605 Rigual-Hernández, A. S., Sierro, F. J., Bárcena, M. A., Flores, J. A., and Heussner, S.:
606 Seasonal and interannual changes of planktic foraminiferal fluxes in the Gulf of Lions (NW
607 Mediterranean) and their implications for paleoceanographic studies: two 12-year sediment trap
608 records, *Deep-Sea Res. Pt. I*, 66, 26–40, doi:10.1016/j.dsr.2012.03.011, 2012.
609 Rouis-Zargouni, I., Turon, J.L., Londeix, L., Essallami, L., Kallel, N., Sicre, M.A.:
610 Environmental and climatic changes in the central Mediterranean Sea (Siculo-Tunisian strait)
611 during the last 30 ka based on dinoflagellate cyst and planktonic foraminifera assemblages.
612 *Palaeogeogr. Palaeoclimatol. Palaeoecol.* 285, 17–29, 2010.
613 Shackleton, N.: Attainment of isotopic equilibrium between ocean water and the
614 benthonic foraminifera genus *Uvigerina*: isotopic changes in the ocean during the last glacial,
615 *CNRS, Colloq. Int.*, 219, 203–209, 1974.
616 Sprovieri, R., Stefano, E. Di, Incarbona, A., and Gargano, M. E.: A high-resolution
617 record of the last deglaciation in the Sicily Channel based on foraminifera and calcareous
618 nannofossil quantitative distribution, *Palaeogeogr. Palaeoecol.*, 202, 119–142, doi:10.1016/S0031-
619 0182(03)00632-1, 2003.
620 Thornalley, D. J. R., Elderfield, H., and McCave, I. N.: Holocene oscillations in
621 temperature and salinity of the surface subpolar North Atlantic., *Nature*, 457, 711–714,
622 doi:10.1038/nature07717, 2009
623 Thunell, R.C.: Distribution of Recent Planktonic Foraminifera in Surface Sediments of
624 the Mediterranean Sea, *Mar. Micropaleontol.*, 3, 147-173, 1978.
625 Yu, J., Elderfield, H., Greaves, M., and Day, J.: Preferential dissolution of benthic
626 foraminiferal calcite during laboratory reductive cleaning, *Geochem. Geophys. Geosy.*, 8, 6,
627 doi:10.1029/2006GC001571, 2007.
628

629

630
631
632
633
634
635

636

637

638

639 **Sea surface temperature variability in the central-western**
640 **Mediterranean Sea during the last 2700 years: a multi-proxy**
641 **and multi-record approach**

642

643 **M. Cisneros¹, I. Cacho¹, J. Frigola¹, M. Canals¹, P. Masqué^{2,3,4}, B. Martrat⁵, [M.](#)
644 [Casado⁵](#), [J. Grimalt⁵](#), [L. D. Pena¹](#), [G. Margaritelli⁶](#) and [F. Lirer⁶](#)**

645 ¹ GRC Geociències Marines, Departament [de Dinàmica de la Terra i de l'Oceà](#), Facultat
646 de Geologia, Universitat de Barcelona, Barcelona, Spain

647 ² Institut de Ciència i Tecnologia Ambientals & Departament de Física, Universitat
648 Autònoma de Barcelona, Bellaterra, Spain

649 ³ School of Natural Sciences and Centre for Marine Ecosystems Research, Edith Cowan
650 University, Joondalup, Australia

651 ⁴ Oceans Institute and School of Physics, The University of Western Australia, Crawley,
652 Australia

653 ⁵ [Institut de Diagnosi Ambiental i Estudis de l'Aigua, Consell Superior d'Investigacions](#)
654 [Científiques, Barcelona, Spain](#)

655 ⁶ Istituto per l'Ambiente Marino Costiero (IAMC)–Consiglio Nazionale delle Ricerche,
656 Calata Porta di Massa, Interno Porto di Napoli, 80133, Napoli, Italy

657 Correspondence to: M. Cisneros (mbermejo@ub.edu)

658 **ABSTRACT**

659 This study analyses the evolution of sea surface conditions during the last 2700 years in
660 the central-western Mediterranean Sea based on six records as measured on five short
661 sediment cores from two sites north of Minorca (cores MINMC06 and HER-MC-MR3).
662 Sea Surface Temperatures (SSTs) were obtained from alkenones and *Globigerina*
663 *bulloides*-Mg/Ca ratios combined with $\delta^{18}\text{O}$ measurements to reconstruct changes in the
664 regional Evaporation–Precipitation (E–P) balance. We reviewed the *G. bulloides*
665 Mg/Ca-SST calibration and re-adjusted it based on a set of core top measurements from
666 the western Mediterranean Sea. According to the regional oceanographic data, the
667 estimated Mg/Ca-SSTs are interpreted to reflect spring seasonal conditions mainly
668 related to the April–May primary productivity bloom. In contrast, the Alkenone-SSTs
669 signal likely integrates the averaged annual signal.

670 A combination of chronological tools allowed synchronizing the records in a
671 common age model. Subsequently a single anomaly stack record was constructed for
672 each proxy, thus easing to identify the most significant and robust patterns. The
673 warmest SSTs occurred during the Roman Period (RP), which was followed by a
674 general cooling trend interrupted by several centennial-scale oscillations. This general
675 cooling trend could be controlled by changes in the annual mean insolation. Whereas
676 some particularly warm SST intervals took place during the Medieval Climate Anomaly
677 (MCA) the Little Ice Age (LIA) was markedly unstable with some very cold SST events
678 mostly during its second half. The records of the last centuries suggest that relatively
679 low E–P ratios and cold SSTs dominated during negative North Atlantic Oscillation
680 (NAO) phases, although SST records seem to present a close positive connection with
681 the Atlantic Multidecadal Oscillation index (AMO).

682

683 1 Introduction

684 | The Mediterranean is regarded as one of the world's highly vulnerable regions with
685 | regard to the current global warming situation (Giorgi, 2006). This high sensitivity to
686 | climate variability has been evidenced in several studies focussed in past natural
687 | changes (Rohling et al., 1998; Cacho et al., 1999a; Moreno et al., 2002; Martrat et al.,
688 | 2004; Reguera, 2004; Frigola et al., 2007; Combourieu Nebout et al., 2009). Paleo-
689 | studies focussed mostly in the rapid climate variability of the last glacial period have
690 | presented solid evidences of a tied connection between changes in North Atlantic
691 | oceanography and climate over the Western Mediterranean Region (Cacho et al., 1999b,
692 | 2000, 2001; Moreno et al., 2005; Sierro et al., 2005; Frigola et al., 2008; Fletcher and
693 | Sanchez-Goñi, 2008). Nevertheless, climate variability during the Holocene and,
694 | particularly during the last millennium, is not so well described in this region, although
695 | its understanding is crucial to place the nature of the 20th century trends in the recent
696 | climate history (Huang, 2004).

697 | Some previous studies have already proposed that Holocene centennial climate
698 | variability in the western Mediterranean Sea could be linked to NAO variability (Jalut et
699 | al., 1997, 2000; Combourieu Nebout et al., 2002; Goy et al., 2003; Roberts et al., 2012;
700 | Fletcher et al., 2012). In particular, nine Holocene episodes of enhanced deep
701 | convection in the Gulf of Lion (GoL) and surface cooling conditions were described at
702 | the same location than this study (Frigola et al., 2007). These events have also been
703 | correlated to intensified upwelling conditions in the Alboran Sea and tentatively
704 | described as two-phase scenarios driven by distinctive NAO states (Ausín et al., 2015).

705 | A growing number of studies reveal considerable climate fluctuations during the last 2
706 | kyr (Abrantes et al., 2005; Holzhauser et al., 2005; Kaufman et al., 2009; Lebreiro et al.,
707 | 2006; Martín-Puertas et al., 2008; Kobashi et al., 2011; Nieto-Moreno et al., 2011,

708 | 2013; Moreno et al., 2012; PAGES 2K Consortium, 2013; Esper et al., 2014; [McGregor](#)
709 | [et al., 2015](#)). However, there is not uniformity about the exact time-span of the different
710 | defined climatic periods such for example the Medieval Climatic Anomaly (MCA),
711 | term coined originally by Stine (1994).

712 | The existing Mediterranean climatic records for the last 1 or 2 kyr are mostly
713 | based on terrestrial source archives such as tree rings (Touchan et al., 2005, 2007;
714 | Griggs et al., 2007; Esper et al., 2007; Büntgen et al., 2011; Morellón et al., 2012),
715 | speleothem records (Frisia et al., 2003; Mangini et al., 2005; Fleitmann et al., 2009;
716 | Martín-Chivelet et al., 2011; Wassenburg et al., 2013), or lake reconstructions (Pla and
717 | Catalan, 2005; Martín-Puertas et al., 2008; Corella et al., 2011; Morellón et al., 2012).
718 | All of these archives can be good sensors of temperature and humidity changes but
719 | often their proxy records mix these two climate variables. Recent efforts have focussed
720 | in integrating these 2 kyr records [into regional](#) climatic signals and they reveal a
721 | complexity in the regional response but also evidence the scarcity of marine records to
722 | have a more complete picture (PAGES, 2009; Lionello, 2012).

723 | In reference to marine records, they are often limited by the lack of adequate
724 | time resolution and accurate chronology to produce detailed comparison with terrestrial
725 | source records, although [they](#) have the potential to provide a wider range of temperature
726 | sensitive proxies. [Currently, few marine-source](#) paleoclimate [records are available](#) from
727 | the last 2 kyr in the Mediterranean Sea (Schilman et al., 2001; Versteegh et al., 2007;
728 | Piva et al., 2008; Taricco et al., 2009, 2015; Incarbona et al., 2010; Fanget et al., 2012;
729 | Grauel et al., 2013; Lirer et al., 2013, 2014; Di Bella et al., 2014; Goudeau et al., 2015)
730 | and they are even more scarce in the Western Basin. The current dispersed data is not
731 | enough to admit a potential common pattern of marine Mediterranean climate
732 | variability for these two millennia (Taricco et al., 2009; Nieto-Moreno et al., 2011;

733 Moreno et al., 2012 and the references therein).

734 The aim of this study is to characterise changes in surface water properties from
735 the Minorca margin in the Catalan-Balearic Sea (central-western Mediterranean),
736 contributing to a better understanding of the climate variations in this region during the
737 last 2.7 kyr. Sea Surface Temperature (SST) has been reconstructed by means of two
738 independent proxies, Mg/Ca analyses on the planktonic foraminifera *Globigerina*
739 *bulloides* and alkenone derived SST (Villanueva et al., 1997; Lea et al., 1999; Barker et
740 al., 2005; Conte et al., 2006). The application of *G. bulloides*-Mg/Ca as a
741 paleothermometer in the western Mediterranean Sea is tested through the analysis of a
742 series of core top samples from different locations of the western Mediterranean Sea
743 and the calibration reviewed consistently. Mg/Ca thermometry is applied with $\delta^{18}\text{O}$ in
744 order to evaluate changes in the Evaporation–Precipitation (E–P) balance of the basin
745 ultimately linked to salinity (Lea et al., 1999; Pierre, 1999; Barker et al., 2005). One of
746 the limitations for the study of climate evolution of the last 2 kyr is that often the
747 intensity of the climate oscillations is at the limit of detection of the selected proxies. In
748 order to identify significant climatic patterns within the proxy records, the analysis have
749 been performed in a collection of multicores from the same region, and their proxy
750 records have been stacked. The studied time periods have been defined as follows
751 (years expressed as BCE=Before Common Era and CE=Common Era): Talaiotic Period
752 (TP; ending at 123 BCE); Roman Period (RP; from 123 BCE to 470 CE); Dark Middle
753 Ages (DMA; from 470 until 900CE); Medieval Climate Anomaly (MCA; from 900 to
754 1275CE); Little Ice Age (LIA; from 1275 to 1850 CE) and Industrial Era (IE) as the
755 most recent period. The limits of these periods are not uniform across the Mediterranean
756 (Lionello, 2012) and here, the selected ages have been chosen according to historical
757 events in Minorca Island and also to the classic climatic ones defined in literature (i.e.

758 Nieto-Moreno et al., 2011, 2013; Moreno et al., 2012; Lirer et al., 2013, 2014).

759 **2 Climatic and oceanographic settings**

760 The Mediterranean Sea is a semi-enclosed basin located in a transitional zone between
761 different climate regimes, from the temperate zone at the north, to the subtropical zone
762 at the south. Consequently, the Mediterranean climate is characterized by mild wet
763 winters and warm to hot, dry summers (Lionello et al., 2006). Interannual climate
764 variability is very much controlled by the dipole-like pressure gradient between the
765 Azores (high) and Iceland (low) system known as the North Atlantic Oscillation (NAO)
766 (Hurrell, 1995; Lionello and Sanna, 2005; Mariotti, 2011; Ausín et al., 2015). But the
767 northern part of the Mediterranean region is also linked to other midlatitude
768 teleconnection patterns (Lionello, 2012).

769 The Mediterranean Sea is a concentration basin (Béthoux, 1980; Lacombe et al.,
770 | 1981) and the excess of evaporation with respect to freshwater input is balanced by
771 | water exchange at the Strait of Gibraltar (i.e. Pinardi and Masetti, 2000; Malanotte-
772 | Rizzoli et al., 2014). The basinwide circulation pattern is prevalently cyclonic (Millot,
773 | 1999). Three convection cells promote the Mediterranean deep and intermediate
774 | circulation: a basinwide open cell and two separated closed cells, one for the Western
775 | Basin and one for the Eastern part. The first one connects the two basins of the
776 | Mediterranean Sea though the Sicilia Strait, where water masses interchange occurs at
777 | intermediate depths. This cell is associated with the inflow of Atlantic Water (AW) at
778 | the Strait of Gibraltar and the outflow of the Levantine Intermediate Water (LIW) that
779 | flows below the first (Lionello et al., 2006).

780 In the north-western Mediterranean Sea, the Northern Current (NC) represents
781 the main feature of the surface circulation transporting waters alongshore from the
782 | Ligurian Sea to the Alboran Sea (Fig. 1a). North-east of the Balearic Promontory a

783 | surface oceanographic front separates Mediterranean waters transported by the NC from
784 | the Atlantic waters that recently entered the Mediterranean (Millot, 1999; Pinot et al.,
785 | 2002; André et al., 2005).

786 | Deep convection occurs offshore the GoL due to the action of very intense cold
787 | and dry winter winds such as the Tramontana and the Mistral. These winds cause strong
788 | evaporation and cooling of surface water thus increasing their density until sinking to
789 | greater depths leading to Western Mediterranean Deep Water (WMDW) (MEDOC,
790 | 1970; Lacombe et al., 1985; Millot, 1999). Dense shelf water cascading (DSWC) in the
791 | GoL also contributes to the sink of large volumes of water and sediments into the deep
792 | basin (Canals et al., 2006).

793 | The north-western Mediterranean is subject to an intense bloom in late winter-
794 | spring when the surface layer stabilizes, and sometimes to a less intense bloom in
795 | autumn, when the strong summer thermocline is progressively eroded (Estrada et al.,
796 | 1985; Bosc et al., 2004; D'Ortenzio and Ribera, 2009; Siokou-Frangou et al., 2010).
797 | SST in the region evolve accordingly with this bloom seasonality, with minima SST in
798 | February, which subsequently increases until maxima summer values during August.
799 | Afterwards, a SST drop can be observed on October although with some interannual
800 | variability (Pastor, 2012).

801 | **3 Material and methods**

802 | **3.1 Sediment cores description**

803 | The studied sediment cores were recovered from a sediment drift built by the action of
804 | the southward branch of the WMDW north of Minorca (Fig. 1). Previous studies carried
805 | out at this site already described high sedimentation rates ($> 20 \text{ cm kyr}^{-1}$) (Frigola et al.,
806 | 2007, 2008; Moreno et al., 2012), which initially suggested a suitable location to carry

807 | on a detailed study of the last millennia. The cores were recovered from two different
808 | stations at about 50 km north of Minorca Island with a multicore system. Cores
809 | MINMC06-1 and MINMC06-2 (henceforth MIN1 and MIN2) (40°29'N, 04°01'E;
810 | 2391m water depth; 31 and 32.5 cm core length, respectively) were retrieved in 2006
811 | during HERMES 3 cruise onboard the R/V Thethys II. In reference to the recovery of
812 | cores HER-MC-MR3.1, HER-MC-MR3.2 and HER-MC-MR3.3 (henceforth MR3.1,
813 | MR3.2 and MR3.3) (40°29'N, 3°37'E; 2117m water depth; 27, 18 and 27 cm core
814 | length, respectively) took place in 2009 during HERMESIONE expedition onboard the
815 | R/V Hespérides. The distance between the MIN and the MR3 cores is ~30 km and both
816 | stations are located in an intermediate position within the sediment drift, which extends
817 | along a water depth range from 2000 to 2700m (Frigola, 2012; Velasco et al., 1996;
818 | Mauffret et al., 1979), being MIN cores deeper than the MR3 ones by about ~300m.

819 | MIN cores were homogeneously sampled at 0.5 cm resolution in the laboratory
820 | while for MR3 cores a different strategy was followed. MR3.1 and MR3.2 were initially
821 | subsampled with a PVC tube and splitted in two halves for XRF analyses in the
822 | laboratory. Both halves of core MR3.1, MR3.1A and MR3.1B, were used for the
823 | present work as replicates of the same core and records for each half are shown
824 | separately. All MR3 cores were sampled at 0.5 cm resolution for the upper 15 cm and at
825 | 1 cm for the rest of the core, with the exception of half MR3.1B that was sampled at
826 | 0.25 cm resolution. MR3 cores were formed by brown-orange nanofossil and
827 | foraminifera silty clay, lightly bioturbated, with the presence of enriched layers in
828 | pteropods and gastropods fragments and some dark layers.

829 | Additionally, core top samples from seven multicores collected at different
830 | locations in the western Mediterranean have also been used for the correction of the
831 | Mg/Ca-SST calibration from *G. bulloides* (Table 1; Fig. 1).

832 3.2 Radiocarbon analyses

833 Twelve ^{14}C AMS dates were performed on cores MIN1, MIN2 and MR3.3 (Table [SI](#),
834 [Suppl. Info.](#)) over 4–22mg samples of planktonic foraminifer *Globigerina inflata*
835 handpicked from the $> 355 \mu\text{m}$ fraction. Ages were calibrated with the standard marine
836 correction of 408 years and the regional average marine reservoir correction (ΔR) for
837 the central-western Mediterranean Sea using Calib 7.0 software (Stuiver and Reimer,
838 1993) and the MARINE13 calibration curve (Reimer et al., 2013).

839 3.3 Radionuclides ^{210}Pb and ^{137}Cs

840 The concentrations of the naturally occurring radionuclide ^{210}Pb were determined in
841 cores MIN1, MIN2, MR3.1A and MR3.2 by alpha-spectroscopy following Sanchez-
842 Cabeza et al. (1998). Concentrations of the anthropogenic radionuclide ^{137}Cs in core
843 MIN1 were measured by gamma spectrometry using a high purity intrinsic germanium
844 detector. Gamma measurements were also used to determine the ^{226}Ra concentrations
845 via the gamma emissions of ^{214}Pb , used to calculate the excess ^{210}Pb concentrations.
846 Sediment accumulation rates for the last century were calculated using the CIC
847 (constant initial concentration) and the CF : CS (constant flux : constant sedimentation)
848 models (Appleby and Oldfield, 1992; Krishnaswami et al., 1971), constrained by the
849 ^{137}Cs concentration profile for core MIN1 (Masqué et al., 2003).

850 3.4 Bulk geochemical analyses

851 The elemental composition of cores MR3.1B and MR3.2 was obtained with a XRF
852 Core-Scanner Avaatech System (CORELAB, University of Barcelona), which is
853 equipped with an optical variable system that allows determining in an independent way
854 the length (10–0.1mm) and the extent (15–2 mm) of the bundle of beams-X. This allows
855 obtaining qualitative information of the elementary composition of the materials. The

856 | core surfaces were scraped cleaned and covered with a 4 μm thin SPEXCertiPrep
857 | Ultralene foil to prevent contamination and minimize desiccation (Richter and van der
858 | Gaast, 2006). Sampling was performed every 1 cm and scanning took place directly at
859 | the split core surface. Among the several measured elements this study has mainly use
860 | the Mn profile in the construction of the age models.

861 | 3.5 Planktonic foraminifera analyses

862 | Specimens for the planktonic foraminifera *Globigerina bulloides* for Mg/Ca and
863 | $\delta^{18}\text{O}$ measurements were picked together from a very restrictive size range (250-355
864 | microns) but then crushed and cleaned separately. In core MR3.1B, picking was often
865 | performed in the $<355 \mu\text{m}$ fraction due to the small amount of material (sampling
866 | every 0.25 cm). Additionally, quantitative analysis of planktonic foraminifera
867 | assemblages was carried out in core MR3.3 and on the upper part of core MR3.1A by
868 | using the fraction size above $125 \mu\text{m}$. The 42 studied samples presented abundant and
869 | well-preserved planktonic foraminifera.

870 | Samples for trace elements analyses were formed by ~45 specimens of *G.*
871 | *bulloides*, crushed under glass slides to open the chambers and carefully cleaned
872 | applying a sequence of clay removal, oxidative and weak acid cleaning steps (Pena et
873 | al., 2005). Only samples from core MR3.1A were cleaned including also the “reductive
874 | step”. Instrumental analyses were performed in an inductively coupled plasma mass
875 | spectrometer (ICP-MS) Perkin Elmer in the Scientific and Technological Centers of the
876 | University of Barcelona (CCiT-UB). A standard solution with a ratio close to the
877 | foraminifera values ($3.2 \text{ mmol mol}^{-1}$) was run every four samples in order to correct any
878 | drift over the measurement runs for MR3.1 halves. Standard solution used on the rest of
879 | analyses was low ($1.6 \text{ mmol mol}^{-1}$). The average reproducibility of Mg/Ca ratios, taking

880 into account the known standard solutions concentrations, was 97 and 89% for MIN1
881 and MIN2 cores, and 99 and 97% for MR3.1A, MR3.1B and MR3.3 cores, respectively
882 Procedure blanks were also routinely measured in order to detect any potential
883 contamination problem during the cleaning and dissolution procedure. Mn/Ca and
884 Al/Ca ratios were always measured in order to detect any potential contamination
885 problem associated with the presence of Mn oxides and aluminosilicates (Barker et al.,
886 2003; Lea et al., 2005; Pena et al., 2005).

887 In order to avoid the overestimation of Mg/Ca-SST by detrital contamination,
888 Mn/Ca values > 0.5 mmol mol⁻¹ were discarded in core MR3.1B and only those higher
889 than 1 mmol mol⁻¹ on MIN1 and MR3.3. With regard to Al/Ca data, those values
890 susceptible of contamination were also removed. After this data cleaning any significant
891 statistical correlation existed between Mg/Ca and Mn/Ca; Al/Ca (r has been always
892 lower than 0.29, p-value=0.06).

893 Mg/Ca ratios were transferred into SST values using the calibration proposed in
894 this study (Sect. 4.1). In the case of the record MR3.1A, cleaned with the reductive
895 procedure, the Mg/Ca ratios were about 23% lower than those measured in core
896 MR3.1B without the reductive step. This ratio lowering is expected from the
897 preferential dissolution of the Mg-enriched calcite during the reductive step (Barker et
898 al., 2003; Pena et al., 2005; Yu et al., 2007). The obtained percentage of Mg/Ca
899 lowering is comparable or higher to those previously estimated for different planktonic
900 foraminifera, although data from *G. bulloides* was not previously reported (Barker et al.,
901 2003). SST-Mg/Ca in core MR3.1A was calculated after the Mg/Ca correction of this
902 23% offset and applying the same calibration than with the other records.

903 Stable isotopes measurements were performed on 10 specimens of *G. bulloides*
904 after sonically cleaned in methanol to remove fine-grained particles. Analyses were

905 performed in a Finnigan-MAT 252 mass spectrometer fitted with a carbonate
906 micro-sampler Kiel-I in the CCiT-UB. Analytical precision of laboratory standards for
907 $\delta^{18}\text{O}$ is better than 0.08 ‰. Calibration to Vienna Pee Dee Belemnite or V-PDB was
908 carried out by means NBS-19 standards (Coplen, 1996).

909 Seawater $\delta^{18}\text{O}$ ($\delta^{18}\text{O}_{\text{sw}}$) was obtained after removing the temperature effect on
910 the *G. bulloides* $\delta^{18}\text{O}$ record by applying the Mg/Ca-SST records in the Shackleton
911 Paleotemperature Equation (Shackleton, 1974). The results are expressed in the water
912 standard SMOW ($\delta^{18}\text{O}_{\text{sw}}$) after the correction of Craig (1965). It was also considered
913 the use of specific temperature equations for *G. bulloides* (Bemis et al., 1998; Mulitza et
914 al., 2003), but the core tops estimates provided $\delta^{18}\text{O}_{\text{sw}}$ values of 2.1 -1.5 SMOW‰,
915 significantly higher than those (~1.2 SMOW‰) measured in water samples from the
916 central-western Mediterranean Sea (Pierre, 1999). Considering that the core top $\delta^{18}\text{O}_{\text{sw}}$
917 estimates, after the application of the empirical Shackleton (1974) paleotemperature
918 equation, averaged 1.1 SMOW‰ and thus closer to the actual water measurements, it
919 was decided that this equation was providing more realistic oceanographical conditions
920 in this location.

921 3.6 Alkenones

922 Measurements of the relative proportion of unsaturated C_{37} alkenones, namely $U^{k'}_{37}$
923 index, were carried out in order to obtain SST records on the studied cores. Detailed
924 information about the methodology and equipment used in C_{37} alkenone determination
925 can be found in Villanueva et al. (1997). The precision of this paleothermometry tool
926 has been determined as close as $\pm 0.5^\circ\text{C}$ (Eglinton et al., 2001). Furthermore, taking
927 into account duplicate alkenone analysis carried out in core MR3.3, the precision
928 achieved results better than $\pm 0.8^\circ\text{C}$. Reconstruction of SST records was based on the

929 | global calibration of Conte et al. (2006), [which considers a estimation standard error of](#)
930 | [1.1°C in surface sediments.](#)

931 | **4 Sea surface temperatures and $\delta^{18}\text{O}$ data**

932 | **4.1 Mg/Ca-SST calibration**

933 | The Mg/Ca ratio measured in *G. bulloides* is a widely used proxy to reconstruct SST
934 | (Barker et al., 2005) although available calibrations can provide very different results
935 | (Lea et al., 1999; Mashiotta et al., 1999; Elderfield and Ganssen, 2000; Anand et al.,
936 | 2003; McConnell and Thunell, 2005; Cl  roux et al., 2008; Thornalley et al., 2009;
937 | Patton et al., 2011). Apparently, the regional Mg/Ca-temperature response varies due to
938 | parameters that have not yet been identified (Patton et al., 2011). A further difficulty
939 | arises from the questioned Mg/Ca-thermal signal in high salinity regions such as the
940 | Mediterranean Sea where anomalous high Mg/Ca values have been observed (Ferguson
941 | et al., 2008). This apparent high salinity sensitivity in foraminifera-Mg/Ca ratios is
942 | under discussion and it has not been supported by recent culture experiments (H  nisch
943 | et al., 2013), which in addition, could be attributed to diagenetic overprints (Hoogakker
944 | et al., 2009; van Raden et al., 2011). In order to test the value of the Mg/Ca ratios in *G.*
945 | *bulloides* from the western Mediterranean Sea and also review its significance in terms
946 | of seasonality and depth habitat, a set of core top samples from different locations of the
947 | western Mediterranean Sea have been analysed. [Core-top samples were recovered using](#)
948 | [a multicorer system and they can be considered as representative of near or present](#)
949 | [conditions \(Masqu   et al., 2003; Cacho et al., 2006\).](#) The studied cores are included in
950 | the 35–45   N latitude range (Table 1 and Fig. 1) and mostly represent two different
951 | trophic regimes, defined by the classical spring bloom (the most north-western basin)
952 | and an intermittently bloom (D'Ortenzio and Ribera, 2009).

953 The obtained Mg/Ca ratios have been compared with the isotopically derived
954 calcification temperatures based on the $\delta^{18}\text{O}$ measurements performed also in *G.*
955 *bulloides* from the same samples. This estimation was performed after applying the
956 Shackleton (1974) paleotemperature equation and using the $\delta^{18}\text{O}_{\text{water}}$ data published by
957 Pierre (1999), taking always into consideration the values of the closer stations and
958 from the top 100 m. The resulting Mg/Ca-SST data have been plotted together with
959 those *G. bulloides* data points from North Atlantic core tops previously published by
960 Elderfield and Ganssen (2000). The resulting high correlation ($r^2 = 0.92$; Fig. 2a)
961 strongly supports the dominant thermal signal in the Mg/Ca ratios of the central-western
962 Mediterranean Sea. Thus, the new data set from the Mediterranean core tops improves
963 the sample coverage over the warm end of the calibration and the resulting exponential
964 function indicates 9.4 % sensitivity in the Mg uptake respect to temperature, which is in
965 agreement with the described range in the literature (i.e., Elderfield and Ganssen, 2000;
966 Barker et al., 2005; Patton et al., 2011). The new calibration obtained from the
967 combination of Mg/Ca-SST data from the western Mediterranean Sea and Atlantic
968 Ocean is:
969
$$\text{Mg} / \text{Ca} = 0.7045(\pm 0.0710)e^{0.0939(\pm 0.0066)T} \quad (1)$$

970 The Mg/Ca-SST signal of *G. bulloides* has been compared with a compilation of water
971 temperature profiles of the first 200 m measured between 1945–2000 yr in stations
972 close to the studied core tops (MEDAR GROUP, 2002). Although significant regional
973 and interannual variations have been observed, the obtained calcification temperatures
974 of our core top samples present the best agreement with temperature values of the upper
975 40 m during the spring months (April–May) (Fig. 2b). This water depth is consistent
976 with that found by plankton tows in the Mediterranean (Pujol and Vergnaud-Grazzini,
977 1995) and with results from multiannual sediment traps monitoring in the Alboran Sea

978 and the GoL where maximum percentages were observed just before the beginning of
979 thermal stratifications (see Bárcena et al., 2004; Bosc et al., 2004; Rigual-Hernández et
980 al., 2012). Although the available information about depth and seasonality distribution
981 of *G. bulloides* is relatively fragmented, this [species](#) is generally situated in intermediate
982 or even shallow waters (i.e. Bé, 1977; Ganssen and Kroon, 2000; Schiebel et al., 2002;
983 Rogerson et al., 2004; Thornalley et al., 2009). However, *G. bulloides* has been also
984 observed at deeper depths in some western Mediterranean Sea sub basins (Pujol and
985 Vergnaud-Grazzini, 1995). Extended data with enhanced spatial and seasonal coverage
986 are required in order to better characterise production, seasonality, geographic and
987 distribution patterns of live foraminifers as *G. bulloides*. Nevertheless, the obtained core
988 top data set offers a solid evidence about the seasonal character of the recorded
989 temperature signal in the Mg/Ca ratio.

990 4.2 A regional stack for SST-Mg/Ca records

991 The obtained Mg/Ca-SST profiles obtained from our sediment records are plotted with
992 the resulting common age model ([see Suppl. Info.](#)) in [Fig. 3](#). The average SST values
993 for the last 2700 years [ranged from \$16.0 \pm 0.9\$ to \$17.8 \pm 0.8\$ °C \(uncertainties of average](#)
994 [values represent \$1\sigma\$; uncertainties of absolute values include analytical precision and](#)
995 [reproducibility and also those derived from Mg/Ca-SST calibration\).](#) All the
996 temperature reconstructions show the warmest sustained period during the RP,
997 approximately between 170 yr BCE to 300 yr CE, except core MIN2, since this record
998 ends at the RP-DA transition. In addition, all the records show a general consistent
999 cooling trend after the RP with several centennial scale oscillations. Maximum Mg/Ca-
1000 SST value is observed in core MR3.3 ([\$19.6 \pm 1.8\$ °C](#)) during the [MCA \(Fig. 3c\)](#) and the
1001 minimum is recorded in core MIN1 ([\$14.4 \pm 1.4\$ °C](#)) during the [LIA \(Fig. 3e\)](#). The

1002 records present high centennial-scale variability. Particularly, during MCA some warm
1003 events reached SST lightly higher than the average of maxima SST (i.e.: $19.6 \pm 1.8^\circ\text{C}$ at
1004 ~ 1021 yr CE). These events were far shorter in duration compared to RP (Fig. 3). The
1005 highest frequency of intense cold events occurred during the LIA and, especially, the
1006 last millennium recorded the minima average Mg/Ca-SST ($15.2 \pm 0.8^\circ\text{C}$). Four of the
1007 five records show a pronounced minima SST after year 1275 CE when occurred the
1008 onset of LIA. In base to the differentiated patterns in Mg/Ca-SST the LIA period has
1009 been divided into two subperiods, an early warmer interval (LIAa) and a later colder
1010 interval (LIAb) with the boundary located at 1540 yr CE.

1011 One of the main difficulties of working with SST reconstructions for the last
1012 millennia is that the targeted climatic signal has often a comparable amplitude to the
1013 internal noise of the records due to sampling and proxy limitations. In order to minimize
1014 this inherent random noise, all the studied records have been combined in a regional
1015 Mg/Ca-SST anomaly stack with the aim to detect the most robust climatic structures
1016 along the different records and reduce the individual noise. Firstly, each SST record was
1017 converted into a SST anomaly record in relation to its average temperature (Fig. 3f).
1018 Secondly, in order to obtain a common sampling interval all records were interpolated.
1019 Although interpolation was performed at 3 different resolutions, results did not differ
1020 substantially (Fig. 3g). Subsequently, we selected the stack that provided the best
1021 resolution offered by our age models (20 yr cm^{-1}) since it preserves very well the high
1022 frequency variability of the individual records (Fig. 3g).

1023 The obtained stack represents in a clearer way the main SST features described
1024 earlier and allows to better identifying the most significant features at centennial-time
1025 scale. Abrupt cooling events are mainly recorded during the LIA (-0.5 to -0.7°C 100 yr^{-1}
1026 1) while abrupt warmings (0.9 to 0.6°C 100 yr^{-1}) are detected during the MCA. Abrupt

1027 [events of similar magnitude have been also obtained during the transition LIA/IE.](#)
1028 [When](#) the whole studied period is considered a long term cooling trend of about [-1 to -](#)
1029 [2°C](#) is observed, however if we focus on the last 1800 yr, since the RP maxima, the
1030 observed cooling trend was far more intense, of about [-3.1 to -3.5°C](#).

1031 [Although the general cooling recorded in our records is very close to the internal](#)
1032 [noise \(-0.3 to -0.8°C kyr⁻¹\), is quite consistent with the recent 2k global reconstruction](#)
1033 [published by McGregor et al., \(2015\) \(best estimation of the SST cooling trend, using](#)
1034 [the average anomaly method 1 for the periods 1-2000 CE: -0.3°C kyr⁻¹ to -0.4°C kyr⁻¹\).](#)

1035 4.3 Oxygen isotope records

1036 Oxygen isotopes measured on carbonates shells of *G. bulloides* ($\delta^{18}\text{O}_c$) and their
1037 derived $\delta^{18}\text{O}_{\text{SW}}$ after removing the temperature effect with Mg/Ca-SST records (see
1038 Sect. 3.5) are shown in [Fig. 4](#). $\delta^{18}\text{O}_c$ and their derived $\delta^{18}\text{O}_{\text{SW}}$ profiles have been
1039 respectively stacked following the same procedure for the SST-Mg/Ca stack (see [Sect.](#)
1040 [4.2](#)). In general terms, all the records present a high stable pattern during the whole
1041 period with a weak depleting trend, which is almost undetectable in some cases (i.e.
1042 core MIN1).

1043 Average $\delta^{18}\text{O}_c$ values [range from 1.2 to 1.4 VPDB‰](#) (and, in general, MR3
1044 cores show lightly heavier values (~ 1.4 [VPDB‰](#)) than MIN cores (~ 1.2 [VPDB‰](#))).
1045 Lightest $\delta^{18}\text{O}_c$ values ([ranged from 1.0 to 1.2 VPDB‰](#)) mostly occur during the RP,
1046 although some short light excursions can be also observed during the end of the MCA
1047 and/or the LIA. Heaviest values ([from 1.4 to 1.8 VPDB‰](#)) are mainly associated with
1048 short events during the LIA, the MCA and over the TP/RP transition. A significant
1049 increase of $\delta^{18}\text{O}_c$ values is observed at the LIA/IE transition, although a sudden drop is
1050 recorded at the end of the stack record (after 1867 yr CE), which could result from a

1051 differential influence of the records (i.e. MIN1) and/or extreme artefact (Fig. 4g).
1052 After removing the temperature effect on the $\delta^{18}\text{O}_c$ record, the remaining $\delta^{18}\text{O}_{\text{SW}}$
1053 record mainly reflects changes in E–P balance, thus resulting as an indirect proxy for
1054 sea surface salinity. The average $\delta^{18}\text{O}_{\text{SW}}$ values obtained for the studied period ranged
1055 from 1.3 to 1.8 ‰. Heaviest $\delta^{18}\text{O}_{\text{SW}}$ values (from 2.4 to 1.9 ‰) are
1056 recorded during the RP when the longest warm period is also observed and some values
1057 are notable during MCA too. Enhancements of the E–P balance ($\delta^{18}\text{O}_{\text{SW}}$ heavier values)
1058 are coincident with higher SST (Fig. 6). Lightest $\delta^{18}\text{O}_{\text{SW}}$ values (from 0.8 to 1.5
1059 ‰) are recorded particularly during the onset and the end of the LIA and also
1060 during the MCA. A drop in the E–P balance has been obtained approximately from the
1061 end of LIA to the most recent years. The most significant changes in our $\delta^{18}\text{O}_{\text{SW}}$
1062 (salinity) stack record correspond to increases in the most recent times and around 1200
1063 yr CE (MCA) and to the decrease observed at the end of the LIA (Fig. 4).

1064 4.4 Alkenone-SST records

1065 The two alkenone ($\text{U}^{k'_{37}}$)-derived SSTs of MIN cores were already published in Moreno
1066 et al. (2012), while the records from MR3 cores are new (Fig. 5). The four Alkenone-
1067 SST records show a similar general cooling trend during the studied period and they
1068 have also been integrated in a SST anomaly stack (Fig. 5e). The whole cooling trend is
1069 of about -1.4°C when the whole studied period is considered and about -1.7°C since the
1070 SST maximum recorded during the RP. Alk-SST absolute values uncertainties in this
1071 section have been estimated to have a mean value of $\pm 1.1^\circ\text{C}$, taking into account the
1072 standard error of estimation (see Sect. 3.6).

1073 Previous studies have interpreted the Alkenone-SST signal in the western
1074 Mediterranean Sea as an annual average (Ternois et al., 1996; Cacho et al., 1999a, b;

1075 Martrat et al., 2004). The average Alkenone-SST values for the studied period (last
1076 2700 yr) ranged from 17.0 to 17.4°C.

1077 The lowest alkenone temperatures (~16.0°C) have been obtained in core MIN2
1078 during the LIAa and the highest (~18.4°C) in core MR3.3 during the MCA. Values
1079 near the average of maxima SST (from 17.9 to 18.4°C) are observed more frequently
1080 during TP, RP and MCA, while temperatures during the onset of MCA and LIA show
1081 many values closer to the average of minima SST (ranged from 16.0 to 16.2°C). The
1082 most abrupt coolings are observed during the LIA and some events were also recorded
1083 during MCA (-0.8°C 100 yr⁻¹) and in less magnitude at the transition LIA/IE (-0.5°C
1084 100 yr⁻¹). The highest warming rates are recorded during the MCA (0.4°C 100 yr⁻¹) and
1085 also during RP.

Eliminado: with the annual mean corresponding to a Balearic site (18.7 ± 1.1°C) according to the integrate values of the upper 50 m (Ternois et al., 1996; Cacho et al., 1999a) of the GCC-IEO database that covers January 1994–July 2008.

1086 4.5 Mg/Ca vs. Alkenone SST records

1087 In this section, Alk uncertainties have been considered as estimation standard error of
1088 1.1°C considered by the calibration used (see Sect. 3.6) and Mg/Ca-SST uncertainties
1089 include analytical precision and reproducibility and also standard error derived from
1090 calibration. The obtained averages of Mg/Ca and Alk derived SST are similar (16.9 ±
1091 1.4°C vs. 17.2 ± 1.1°C), but the temperature range of the Mg/Ca records shows higher
1092 amplitude (see Sect. 4.2 and 4.4).

1093 The enhanced Mg/Ca-SST variability is also reflected in the short-term
1094 oscillations, at centennial time scale, which are better represented in the Mg/Ca record
1095 with oscillations over 0.5°C, while in the alkenone record are shorter. This difference in
1096 the signal amplitude cannot be attributed to the different habitat depth since alkenones
1097 should reflect the surface photic layer (<50 m), while *G. bulloides* has the capability to
1098 develop in a wider and deeper environment (Bé, 1977; Pujol and Vergnaud-Grazzini,

1105 1995; Ternois et al., 1996; Sicre et al., 1999; Ganssen and Kroon, 2000; Schiebel et al.,
1106 2002; Rogerson et al., 2004; Thornalley et al., 2009), where less changes would be
1107 expected. This enhanced Mg/Ca-SST variability could be attributed to the highly
1108 restricted seasonal character of its signal, which purely reflects SST changes during the
1109 spring season. However, the coccolith signal integrates a wider time period from
1110 autumn to spring (Rigual-Hernández et al., 2012, 2013) and, consequently, changes
1111 associated with specific seasons become more diluted in the resultant averaged signal.

1112 The annual mean corresponding to a Balearic site according to the integrate
1113 values of the upper 50 m (Ternois et al., 1996; Cacho et al., 1999a) of the GCC-IEO
1114 database that covers January 1994–July 200 is $18.7 \pm 1.1^\circ\text{C}$. Our core tops records,
1115 which represent the last decades, show SST values closer to the annual mean in the case
1116 of Alk-SST than Mg/Ca-SST that recorded slightly lower values.

1117 U^k₃₇-SST records in the western Mediterranean Sea have been interpreted to
1118 represent mean annual SST (i.e. Cacho et al., 1999a; Martrat et al., 2004) but seasonal
1119 variations in alkenone production could play an important role in the U^k₃₇-SST values
1120 (Rodrigo-Gámiz et al., 2014). Considering that during the summer months the
1121 Mediterranean Sea is a very stratified and oligotrophic sea, it should be expected
1122 reduced alkenone production during this season (Ternois et al., 1996; Sicre et al., 1999;
1123 Bárcena et al., 2004; Versteegh et al., 2007; Hernández-Almeida et al., 2011). This
1124 observation is further supported by the results from sediment traps located in the GoL
1125 showing very low coccolith fluxes during the summer months (Rigual-Hernández et al.,
1126 2013), while they show higher values during autumn, winter and spring, reaching
1127 maximum values at the end of the winter season, during SST minima. In contrast, high
1128 fluxes of *G. bulloides* are almost restricted to the upwelling spring signal, when
1129 coccolith fluxes have already started to decrease (Rigual-Hernández et al., 2012, 2013).

1130 This different growth season can explain the proxy bias in the SST reconstructions, with
1131 more diluted SST signal recorded by the alkenones.

1132 Both Mg/Ca-SST and U^k₃₇-SST records show a consistent cooling trend during
1133 the studied period (2700 yr) of about -0.5°C kyr⁻¹ which is consistent with the recent 2k
1134 global reconstruction published by McGregor et al., (2015) (see Sect. 4.2). The recorded
1135 cooling since the RP maxima (~200 yr CE) is more pronounced in the Mg/Ca-SST (-1.7
1136 to -2.0°C kyr⁻¹) than in the Alkenone record (-1.1°C kyr⁻¹). These coolings are larger
1137 than those estimated in the global reconstruction (McGregor et al., 2015) for the last
1138 1200 yr (average anomaly method 1: -0.4°C kyr⁻¹ to -0.5°C kyr⁻¹). It should be noted
1139 that the global reconstruction includes Alk-SST from MIN cores (data published in
1140 Moreno et al., 2012).

1141 The detailed comparison of the centennial SST variability recorded by both
1142 proxy stacks consistently indicates a puzzling antiphase (Fig. 11b and c). Although the
1143 main trends are consistently parallel in both alkenone and Mg/Ca proxies ($r=0.5$; p
1144 value=0) as has been noted in other regions, short-term variability appears to have an
1145 opposite character. Results obtained by means of Welch's test indicate that the null
1146 hypothesis (means are equal) can be discarded at the 5% error level: t_{observed}
1147 (12.446) > t_{critical} (1.971). This unexpected outcome is a firm evidence of the relevance of
1148 the seasonal variability in the climate evolution and would indicate that extreme winter
1149 coolings were followed by a more rapid and intense spring warmings. Nevertheless,
1150 regarding the low amplitude of several of these oscillations, often close to the error of
1151 the proxies, this observation needs to be probed with further constraints as a solid regional
1152 feature.

1153 5 Discussion

1154 5.1 Climate patterns during the last 2.7 kyr

1155 Changes in SST in the Minorca region have implications in the surface air mass
1156 temperature and moisture source regions that would determine air mass trajectories and
1157 ultimately precipitation regime in the Western Mediterranean Region (Millán et al.,
1158 2005; Labuhn et al., 2015). Observations of recent data have identified SST as a key
1159 factor in the development of torrential rain events in the Western Mediterranean Basin
1160 (Pastor et al., 2001), being able to act as a source of potential instability of air masses
1161 that transit over these waters (Pastor, 2012). In this line, the combination of SST
1162 reconstruction with $\delta^{18}\text{O}_{\text{sw}}$ can provide a light to analyse the connection between
1163 thermal changes and moisture export from the central-western Mediterranean Sea
1164 during the last 2.7 kyr.

1165 The older period recorded by our records is the so-call Talaiotic Period (TP),
1166 which corresponds to the Ancient Ages as the Greek Period in other geographic areas.

1167 Both studied SST proxies are consistent showing a general cooling trend from ~500 yr
1168 BCE and reaching minimum values by the end of the period (~120 yr BCE),
1169 synchronously with a reduction in the E-P rate occurred (Fig. 6a-c). Very few other
1170 records exist from this time period to compare these trends at regional scale.

1171 One of the most outstanding features in the two SST-reconstructions,
1172 particularly in the Mg/Ca-SST stack is the warm SST that dominated especially during
1173 the second half of the RP (150–400 yr CE). The onset of the RP was relatively cold and
1174 a ~2°C warming occurred during the first part of this period. This SST evolution from
1175 colder to warmer conditions during the RP is consistent with the isotopic record from
1176 the Gulf of Taranto (Taricco et al., 2009) and peat reconstructions from north-western

1177 Spain (Martínez-Cortizas et al., 1999), and to some extent to SST proxies in the SE
1178 Tyrrhenian Sea (Lirer et al., 2014). However none of these records indicate that the RP
1179 was the warmest period of the last 2 kyr. Other records from higher latitudes such as
1180 Greenland (Dahl-Jensen et al., 1998), North Europe (Esper et al., 2014), North Atlantic
1181 Ocean (Bond et al., 2001; Sicre et al., 2008), speleothem records from North Iberia
1182 (Martín-Chivelet et al., 2011) and even the multiproxy PAGES 2K reconstruction from
1183 Europe, suggest a rather warmer early RP than late RP and, again, none of these records
1184 highlights the roman times as the warmest climate period of the last 2 kyr.
1185 Consequently, these very warm RP conditions recorded in the Minorca Mg/Ca-SST
1186 stack appears to have a very regional character and suggest a rather heterogeneous
1187 thermal response along the European continent and surrounding marine regions.

1188 According to the $\delta^{18}\text{O}_{\text{sw}}$ -stack the RP seems to be accompanied by an increase
1189 | in the E–P ratio (Fig. 6a) as also has been observed in some close regions as Alps
1190 | (Holzhauser et al., 2005; Joerin et al., 2006). But a lake record from Southern Spain
1191 | indicates relatively high levels when $\delta^{18}\text{O}_{\text{sw}}$ stack indicates the maximum in E–P ratio
1192 | (Martín-Puertas et al., 2008). This information is not necessarily contradictory, since
1193 | enhanced E–P balance in the Mediterranean could induce enhanced precipitation in
1194 | some of the regions, but more detailed geographical information should be required to
1195 | really evaluate such situation.

1196 After the RP, during the whole DMA and until the MCA, Mg/Ca-SST stack
1197 | shows a cooling of $\sim 1^\circ\text{C}$ (-0.2°C 100 yr^{-1}), which is of 0.3°C in the case of the
1198 | Alkenone-SST stack; E–P rate is also decreasing. This trend is in contrast with the
1199 | general warming trend interpreted in speleothem records from the North Iberia (Martín-
1200 | Chivelet et al., 2011) or the transition towards drier conditions discussed from Alboran
1201 | recods (Nieto- Moreno et al., 2011). SST proxies from the Tyrrhenian Sea show a

1202 | [cooling trend after](#) the second half of the DMA and the Roman IV cold/dry phase
1203 | described by Lirer et al. (2014) [that](#) can be tentatively correlated [with our SST records](#)
1204 | ([Fig. 6](#)). This cooling phase is also documented in $\delta^{18}\text{O}_{G. ruber}$ record of Gulf of Taranto
1205 | by Grauel et al. (2013). The heterogeneity of the signal in the [different](#) proxies and
1206 | regions reveals the difficulty to characterise the climate variability during these short
1207 | periods and reinforce the need of better geographical coverage of individual proxies.

1208 | Frequently, the Medieval Period is described as a very warm period in numerous
1209 | regions in the Northern Hemisphere (Hughes and Diaz, 1994; Mann et al., 2008;
1210 | Martín-Chivelet et al., 2011), but an increasing number of studies are questioning the
1211 | existence of such a “warm” period (i.e. Chen et al., 2013). Minorca SST-stacks also
1212 | indicate variable temperatures and it does not stand as a particular warm period within
1213 | the last 2 kyr ([Fig. 6](#)). A significant warming event is centred at [~1000 yr CE](#) and a later
1214 | cooling with minimum values at about 1200 yr CE ([Fig. 6](#)). Higher variability is found
1215 | in Greenland record (Kobashi et al., 2011) while an early warm MCA and posterior
1216 | cooling is also observed in temperature reconstructions from Central Europe (Büntgen
1217 | et al., 2011) and also the European multi-proxy 2k stack for PAGES 2K Consortium
1218 | (2013). But all these proxies agree in indicating overall warmer temperatures during the
1219 | MCA than during the LIA. At the MCA/LIA transition a progressive cooling and a
1220 | change in cyclic oscillation before and after the onset of LIA are visible. This transition
1221 | is considered the last rapid climate change (RCC) of Mayewski et al. (2004).

1222 | In the context of the Mediterranean Sea, lake, marine and speleothem proxies
1223 | suggest drier conditions during the MCA than during the LIA (Moreno et al., 2012;
1224 | Chen et al., 2013; Nieto-Moreno et al., 2013; Wassenburg et al., 2013). Looking to the
1225 | $\delta^{18}\text{O}_{sw}$ stack, several oscillations are observed during the MCA and LIA but any clear
1226 | differentiation between the MCA and LIA can be inferred from this proxy, indicating

1227 that these reduced precipitation also involved reduced evaporation in the basin without
1228 altering the E–P balance recorded by the $\delta^{18}\text{O}_{\text{sw}}$ proxy. The centennial scale variability
1229 detected in both the Mg/Ca-SST stack and $\delta^{18}\text{O}_{\text{sw}}$ stack reveal that higher E–P
1230 conditions existed during the warmer intervals ([Fig. 6a and c](#)).

1231 The LIA stands as a period of high thermal variability according to the Mg/Ca-
1232 SST stack and, in base to these records, two substages can be differentiated, a first one
1233 when SST oscillations were larger and average temperatures warmer (LIAa) and a
1234 second one with shorter oscillations and colder average SST (LIAb). We suggest that
1235 LIAa interval could be linked to the Wolf and Spörer solar minima and LIAb
1236 corresponds to Maunder and Dalton cold events, [in agreement with previous](#)
1237 [observations \(i.e. Vallefuoco et al., 2012\)](#).

1238 Furthermore, the two LIA substages are also present in the Greenland record
1239 (Kobashi et al., 2011). The intense cooling drop ($0.8^{\circ}\text{C } 100 \text{ yr}^{-1}$) at the onset of the
1240 LIAb is in agreement with the suggested coolings of 0.5 and 1°C in the Northern
1241 Hemisphere (i.e. Matthews and Briffa, 2005; Mann et al., 2009). The described two
1242 steps within the LIA are clearer in the Mg/Ca-SST stack than in the Alkenone-SST
1243 stack; this is also the case of the alkenone records in Alboran Sea (Nieto-Moreno et al.,
1244 2011) and [it](#) may be consequence of the general reduced SST variability detected by
1245 these proxies (see Sect. [4.5](#)).

1246 In terms of humidity, the LIA is described as a period of increased runoff
1247 according to the Alboran record (Nieto-Moreno et al., 2011). The available lake level
1248 reconstruction from South Spain also reveals a progressive increase after the MCA,
1249 reaching a maximum during the LIAb (Martín-Puertas et al., 2008). Different records of
1250 flood events in the Iberia Peninsula also report a significant increase of extreme events
1251 during the LIA (Barriendos et al., 1998; Benito et al., 2003; Moreno et al., 2008). These

1252 conditions are consistent with the described enhanced storm activity over the GoL for
1253 the LIA (Sabatier et al., 2012). These conditions could account for the enhanced
1254 humidity transport towards the Mediterranean Sea that could produce the reduced E–P
1255 ratio detected in the $\delta^{18}\text{O}_{\text{sw}}$ particularly for the LIAb (Fig. 6a).

1256 The end of the LIA and onset of the IE is marked in the Mg/Ca-SST stack with a
1257 warming phase of about 1°C and less pronounced in the Alkenone-SST stack. This
1258 initial warm climatic event is also documented in other Mediterranean regions (Taricco
1259 et al., 2009; Marullo et al., 2011; Lirer et al., 2014) and Europe (PAGES 2K
1260 Consortium, 2013), which is coincident with a Total Solar Irradiance (TSI)
1261 enhancement after Dalton Minima. The two Minorca SST stacks show a cooling trend
1262 by the end of the record, which does not seem coherent with the instrumental
1263 atmospheric records. In Western Mediterranean, warming has been registered in two
1264 main phases: from the mid-1920s to 1950s and from the mid-1970s onwards (Lionello
1265 et al., 2006). The Minorca stacks do not show such a warming although they do not
1266 cover the second period of warming. Nevertheless, according to instrumental data from
1267 the upper layer on the Western Mediterranean since the beginning of the XX century, no
1268 warming trends were detected before the 1980s (Vargas-Yáñez et al., 2010).

1269 5.2 Climate forcing mechanisms

1270 The general cooling trend observed in both Mg/Ca-SST and Alkenone-SST stacks
1271 presents a good correlation with the summer insolation evolution in the North
1272 Hemisphere, which actually dominates the annual insolation balance ($r=0.2$ and 0.8 , p
1273 value ≤ 0.007 , respectively) (Fig. 7). This external forcing has already been proposed to
1274 control major SST trends for the whole Holocene period in numerous records from
1275 Northern Hemisphere (i.e. Wright, 1994; Marchal et al., 2002; Kaufman et al., 2009;
1276 Moreno et al., 2012). Also summer insolation seems to have had a significant influence

1277 | in the decreasing trend obtained in the isotope records during the whole spanned period
1278 | (r=0.4, p value=0) as has been suggested in the study of Ausín et al. (2015), among
1279 | others. Nevertheless, another forcing needs to account for the centennial-scale
1280 | variability of the records, as could be the higher volcanism in the last millennium
1281 | (McGregor et al., 2015) although no significant correlations have been obtained
1282 | between our records and volcanic reconstructions (Gao et al., 2008).

1283 | Solar variability has frequently been suggested as a primary driver of the
1284 | Holocene millennial-scale variability (i.e. Bond et al., 2001). Several oscillations can be
1285 | observed in the TSI record (Fig. 7a) whose correlation with the Mg/Ca-SST and
1286 | Alkenone-SST stacks are low, since most of the major drops in TSI does not correspond
1287 | to SST cold events; although in the case of the Alkenone-SST stack some degree of
1288 | correlation exists between the two records (r=0.5, p value=0). Nevertheless, TSI does
1289 | not seem to be the primer driver of the centennial scale SST variability in the studied
1290 | records.

1291 | Furthermore, one of the major drivers of Mediterranean inter-annual variability
1292 | in the Mediterranean region is the NAO (Hurrell, 1995; Lionello and Sanna, 2005;
1293 | Mariotti, 2011). High state of the NAO produces high pressure over the Mediterranean
1294 | Sea inducing an increment of the E–P balance and reduces sea level over several sectors
1295 | of the Mediterranean Sea (Tsimplis and Josey, 2001). During these positive NAO
1296 | periods, winds over the Mediterranean enhance their north direction, overall salinity
1297 | increases and formation of dense deep water masses is reinforced as the water exchange
1298 | through the Corsica channel while the arrival of north storm waves decreases (Wallace
1299 | and Gutzler, 1981; Tsimplis and Baker, 2000; Lionello and Sanna, 2005). The effect of
1300 | NAO on Mediterranean temperatures is more ambiguous. Changes during the last
1301 | decades does not show significant variability with NAO (Luterbacher, 2004; Mariotti,

1302 2011) although some studies suggest an opposite response between the two basins with
1303 cooling responses in some eastern basins and warming in the western during positive
1304 NAO conditions (Demirov and Pinardi, 2002; Tsimplis and Rixen, 2002). Although still
1305 controversial, some NAO reconstructions on proxy-records start to be available for the
1306 studied period (Lehner et al., 2012; Olsen et al., 2012; Trouet et al., 2012; Ortega et al.,
1307 2015). The last millennium is the best-resolved period and that allows a direct
1308 comparison with our data to evaluate the potential link to NAO.

1309 The correlations between our Minorca temperatures stacks with NAO
1310 reconstructions (Fig. 7) are relatively low in the case of Mg/Ca-SST ($r=0.3$, p
1311 $value \leq 0.002$) and not significant in the Alkenone stack, indicating that this forcing is
1312 probably not the driver of the main trends in the records, although several uncertainties
1313 still exist about the long NAO reconstructions (Lehner et al., 2012). Notwithstanding
1314 the relatively low correlation between NAO with Mg/Ca-SST, when a detailed analysis
1315 is done focussing on the more intense negative NAO phases, those below 0 (Fig. 7),
1316 they mostly appear to correlate with cooling phases in the Mg/Ca-stack. The frequency
1317 of these negative events is particularly high during the LIA, and mostly during its
1318 second phase (LIAb) when the coldest intervals of our SST-stacks occurred.

1319 When the last centuries are compared in detail with the last NAO reconstruction
1320 based on several different proxy records of annual resolution and tested with some
1321 model assimilations (Ortega et al., 2015), the obtained correlations between $\delta^{18}O_{sw}$ and
1322 NAO are not statistically significant. But Welch's test results indicate that the null
1323 hypothesis (difference between means is 0) cannot be discarded for both proxies, given
1324 that calculated p-value (0.913) is higher than the significance level alpha (0.05) ($t_{observed}$
1325 $= -0.109 < t_{critical} = 1.960$). During the last centuries it can be observed a coherent
1326 pattern of variability with our $\delta^{18}O_{sw}$ reconstruction, with high (low) isotopic values

1327 | mainly dominating during positive (negative) NAO phases (Fig. 8). This picture is
1328 | coherent with the described increase in the E–P balance during high NAO phases
1329 | described for the last decades (Tsimplis and Josey, 2001), which would also contribute
1330 | to the concentration of the ^{18}O in the Mediterranean waters. The SST stacks also suggest
1331 | some degree of correlation between warm SST and high NAO values (Fig. 7) but a more
1332 | coherent picture is observed when the SST-records are compared to the AMO
1333 | reconstruction: warm SST dominated during high AMO values (Fig. 9). This picture of
1334 | salinity changes related to NAO and SST to AMO has actually been also described in
1335 | base to the analysis of last decades data (Mariotti, 2011; Guemas et al., 2014) and
1336 | confirms the complex but tied response of the Mediterranean to atmospheric and marine
1337 | changes over the North Atlantic Ocean.

1338 | The pattern of high $\delta^{18}\text{O}_{\text{SW}}$ when dominant positive NAO conditions occurred
1339 | should indicate a reduction in the humidity transport over the Mediterranean region as a
1340 | consequence of the high atmospheric pressure conditions (Tsimplis and Josey, 2001).
1341 | To test this hypothesis, the $\delta^{18}\text{O}_{\text{SW}}$ stack and the NAO reconstruction is compared to a
1342 | proxy interpreted to reflect storm intensity over the GoL (Fig. 8), also linked to
1343 | increased storm activity in the Eastern North Atlantic (Sabatier et al., 2012). Several
1344 | periods of increased/decreased storm activity in the GoL correlate indeed with low/high
1345 | values in the $\delta^{18}\text{O}_{\text{SW}}$ supporting that during negative NAO conditions North European
1346 | storm waves can more frequently arrive into the Mediterranean Sea (Lionello and
1347 | Sanna, 2005), contributing to the reduction of the E–P balance (Fig. 8). This data
1348 | comparison would also support that during these enhanced storm periods, cold SST
1349 | conditions would dominate in the region as has been previously suggested (Sabatier et
1350 | al., 2012). Nevertheless, not all the NAO oscillations had identical expression in the
1351 | compared records and it is coherent with recent observations negative NAO phases that

1352 | [present different](#) atmospheric configuration modes and thus impact over the western
1353 | Mediterranean Sea (Sáez de Cámara et al., in proof, 2015). [Regarding the lower part of](#)
1354 | [the record](#), the maximum SST temperatures and $\delta^{18}\text{O}_{\text{SW}}$ recorded during the RP (100–
1355 | 300 yr CE) may suggest the occurrence of persistent positive NAO conditions, which
1356 | would also be consistent with a high pressure driven drop in relatively sea level as has
1357 | been reconstructed in the north-western Mediterranean Sea (Southern France) (-40 ± 10
1358 | cm) (Morhange et al., 2013).

1359 | It is interesting to note that during the DMA a pronounced and intense cooling event is
1360 | recorded in the Mg/Ca-SST stack at about 500 yr CE. Several references document in
1361 | the scientific literature the occurrence of the so-called dimming of the sun at 536–537 yr
1362 | CE (Stothers, 1984). This event, in base to ice core records, has been able to be linked a
1363 | tropical volcanic eruption (Larsen et al., 2008). Tree-ring data reconstructions from
1364 | Europe and also historical documents indicate the persistence during several years
1365 | (536–550 yr CE) of what is described as the most severe cooling across the Northern
1366 | Hemisphere during the last two millennia (Larsen et al., 2008). Despite the limitations
1367 | derived from the resolution of our records, Mg/Ca-SST stack record may have caught
1368 | this cooling and that would prove the robustness of our age models.

1369 | **6 Summary and conclusions**

1370 | The review of new core top data of *G. bulloides*-Mg/Ca ratios from the central-western
1371 | Mediterranean Sea together with previous published data support a consistent
1372 | temperature sensitivity for the Mediterranean samples and allows to refine the
1373 | previously calibrations. The recorded Mg/Ca-SST signal from *G. bulloides* is
1374 | interpreted to reflect April–May conditions from the upper 40m layer. In contrast, the
1375 | Alkenone-SST estimations are interpreted to integrate a more annual averaged signal,

1376 although biased toward the winter months since primary productivity during the
1377 summer months in the Mediterranean Sea is extremely low. This more averaged signal
1378 of the Alkenone-SST records may explain why they present more smoothed oscillations
1379 in comparison to the Mg/Ca-SST records.

1380 After the careful construction of a common chronology for the studied
1381 multicores, in base to several chronological tools, the individual proxy records have
1382 been joined in an anomaly-stacked record to allow a better identification of the more
1383 solid patterns and structures. Both Mg/Ca-SST and Alkenone stacks show a consistent
1384 cooling trend over the studied period and since the Roman Period maxima this cooling
1385 is -1.7 to -2.0°C kyr⁻¹ in the Mg/Ca record and less pronounced in the alkenones record
1386 (-1.1°C kyr⁻¹). This cooling trend seems to be consistent with the general lowering in
1387 summer insolation. This general cooling trend is punctuated by several SST oscillations
1388 at centennial time scale, which represent: maximum SST dominated during most of the
1389 Roman Period (RP); a progressive cooling during Dark Middle Ages (DMA);
1390 pronounced variability during Medieval Climate Anomaly (MCA) with two intense
1391 warming phases reaching warmer SST than during Little Ice Age (LIA); and very
1392 unstable and rather cold LIA, with two substages, a first one with larger SST
1393 oscillations and warmer average temperatures (LIAa) and a second one with shorter
1394 oscillations and colder average SST (LIAb). The described two stages within the LIA
1395 are clearer in the Mg/Ca-SST stack than in the Alkenone-SST record. Comparison of
1396 Mg/Ca-SST and $\delta^{18}\text{O}_{\text{sw}}$ stacks indicates that warmer intervals have been accompanied
1397 by higher Evaporation–Precipitation (E–P) conditions. The E–P balance oscillations
1398 over each defined climatic period during the last 2.7 kyr suggest variations in the
1399 thermal change and moisture export patterns in the central-western Mediterranean.

1400 The comparison of the Minorca SST-stacks with other paleoclimatic records

1401 form Europe suggests a rather heterogonous thermal response along the European
1402 continent and surrounding marine regions. Comparison of the new Mediterranean
1403 records with the reconstructed variations in Total Solar Irradiance (TSI) does not
1404 support a clear connection with this climate forcing. Nevertheless, changes in the North
1405 Atlantic Oscillation (NAO) and Atlantic Multidecadal Oscillation (AMO) seem to have
1406 exerted a more relevant role controlling climate changes in the region. The negative
1407 NAO phases appear to correlate mostly with cooling phases in the Mg/Ca-stack,
1408 although this connection is complex and apparently clearer during the most intense
1409 negative phases. Nevertheless, when the comparison is focussed in the last 1 kyr, when
1410 NAO reconstructions are better constrained, a more consistent pattern arises, with cold
1411 and particularly fresher $\delta^{18}\text{O}_{\text{SW}}$ values (reduced E-P balance) during negative NAO
1412 phases. A picture of enhanced southward transport of European storm tracks during this
1413 period would be coherent with the new data and previous reconstructions of storm
1414 activity in the GoL. Nevertheless, the SST-stacks seem to present a more tied relation to
1415 AMO during the last four centuries (the available period of AMO reconstructions):
1416 warm SST dominated during high AMO values. These evidences would support a close
1417 connection between Mediterranean and North Atlantic oceanography for the last 2 kyr.

1418 *Acknowledgements.* Cores MINMC06 were recovered by HERMES 3 cruise in 2006 on
1419 R/V Thethys II and HER-MC-MR3 cores were collected by HERMESIONE expedition
1420 on board of R/V Hespérides in 2009. This research has financially been supported by
1421 OPERA (CTM2013-48639-C2-1-R). We thank Generalitat de Catalunya Grups de
1422 Recerca Consolidats grant 2009 SGR 1305 to GRC Geociències Marines. [Project of](#)
1423 [Strategic Interest NextData PNR 2011-2013 \(www.nextdatapoint.it\)](#) has also
1424 [collaborated in the financing.](#) We are grateful to M. Guart (Dept. d'Estratigrafia,
1425 Paleontologia i Geociències Marines, Universitat de Barcelona), M. Romero, T. Padró
1426 and J. Perona (Serveis Científico-Tècnics, Universitat de Barcelona), J.M. Bruach
1427 (Departament de Física, Universitat Autònoma de Barcelona) [and B. Hortelano, Y.](#)
1428 [Gonzalez-Quinteiro and I. Fernández \(Institut de Diagnosi Ambiental i Estudis de](#)
1429 [l'Aigua, CSIC, Barcelona\)](#) for their help with the laboratory work, D. Amblàs for his
1430 collaboration with the artwork of maps and to Paleoteam for the unconditional support.
1431 [E. Garcia-Solsona](#), S. Giralt and M. Blaauw are acknowledged for their help. [B. Martrat](#)
1432 [acknowledges funding from CSIC-Ramon y Cajal post-doctoral program RYC-2013-](#)
1433 [14073.](#) [M. Cisneros](#) benefited from a fellowship of the University of Barcelona. [I.](#)
1434 [Cacho thanks the ICREA-Academia program form the Generalitat de Catalunya.](#)

1435 **References**

- 1436 Abrantes, F., Lebreiro, S., Rodrigues, T., Gil, I., Bartels-Jónsdóttir, H., Oliveira, P.,
1437 Kissel, C., and Grimalt, J. O.: Shallow-marine sediment cores record climate
1438 variability and earthquake activity off Lisbon (Portugal) for the last 2000 years,
1439 *Quaternary Sci. Rev.*, 24, 2477–2494, doi:10.1016/j.quascirev.2004.04.009, 2005.
- 1440 Anand, P., Elderfield, H., and Conte, M. H.: Calibration of Mg/Ca thermometry in
1441 planktonic foraminifera from a sediment trap time series, *Paleoceanography*, 18,
1442 1050, doi:10.1029/2002PA000846, 2003.
- 1443 André, G., Garreau, P., Garnier, V., and Fraunié, P.: Modelled variability of the sea
1444 surface circulation in the North-western Mediterranean Sea and in the Gulf of Lions,
1445 *Ocean Dynam.*, 55, 294–308, 2005.
- 1446 Appleby, P. G. and Oldfield, F.: *Application of Lead-210 to Sedimentation Studies*,
1447 Clarendon Press, Oxford, Chapt. 21, 731–778, 1992.
- 1448 Ausín, B., Flores, J. A., Sierro, F. J., Cacho, I., Hernández-Almeida, I., Martrat, B., and
1449 Grimalt, J. O.: Atmospheric patterns driving Holocene productivity in the Alboran
1450 Sea (Western Mediterranean): a multiproxy approach, *The Holocene*, 25, 1–13,
1451 doi:10.1177/0959683614565952, 2015.
- 1452 Bárcena, M. A., Flores, J. A., Sierro, F. J., Pérez-Folgado, M., Fabres, J., Calafat, A.,
1453 and Canals, M.: Planktonic response to main oceanographic changes in the Alboran
1454 Sea (Western Mediterranean) as documented in sediment traps and surface
1455 sediments, *Mar. Micropaleontol.*, 53, 423–445,
1456 doi:10.1016/j.marmicro.2004.09.009, 2004.
- 1457 Barker, S., Greaves, M., and Elderfield, H.: A study of cleaning procedures used for
1458 foraminiferal Mg/Ca paleothermometry, *Geochem. Geophys. Geosy.*, 4, 9,
1459 doi:10.1029/2003GC000559, 2003.
- 1460 Barker, S., Cacho, I., Benway, H., and Tachikawa, K.: Planktonic foraminiferal Mg/Ca
1461 as a proxy for past oceanic temperatures: a methodological overview and data
1462 compilation for the Last Glacial Maximum, *Quaternary Sci. Rev.*, 24, 821–834,
1463 doi:10.1016/j.quascirev.2004.07.016, 2005.
- 1464 Barriendos, M. and Martín-Vide, J.: Secular climatic oscillations as indicated by
1465 catastrophic floods in the Spanish Mediterranean coastal area (14th–19th centuries),
1466 *Clim. Change*, 38, 473–491, 1998.
- 1467 Bé, A. W. H. and Hutson, W. H.: Ecology of planktonic foraminifera and biogeographic
1468 patterns of life and fossil assemblages in the Indian Ocean, *Micropaleontology*, 23,
1469 369–414, 1977.
- 1470 [Bemis, B. E., Spero, H. J., Bijma, J. and Lea, D. W.: Reevaluation of the oxygen](#)
1471 [isotopic composition of planktonic foraminifera: Experimental results and revised](#)
1472 [paleotemperature equations, *Paleoceanography*, 13\(2\), 150–160,](#)
1473 [doi:10.1029/98PA00070, 1998.](#)
- 1474 Benito, G., Sopeña, A., Sánchez-Moya, Y., Machado, M. J., and Pérez-González, A.:
1475 Palaeoflood record of the Tagus River (Central Spain) during the Late Pleistocene
1476 and Holocene, *Quaternary Sci. Rev.*, 22, 1737–1756, doi:10.1016/S0277-
1477 3791(03)00133-1, 2003.
- 1478 Béthoux, J. P.: Mean water fluxes across sections in the Mediterranean Sea, evaluated in
1479 the basis of water and salt budgets and of observed salinities, *Oceanol. Acta*, 3, 79–
1480 88, 1980.
- 1481 Blaauw, M. and Christen, J. A.: Flexible paleoclimate age-depth models using an
1482 autoregressive gamma process, *Bayesian Anal.*, 6, 457–474, doi:10.1214/11-BA618,
1483 2011.
- 1484

- 1485 Bond, G., Kromer, B., Beer, J., Muscheler, R., Evans, M. N., Showers, W., Hoffmann,
 1486 S., Lottibond, R., Hajdas, I., and Bonani, G.: Persistent solar influence on North
 1487 Atlantic climate during the holocene, *Science*, 294, 2130–2136,
 1488 doi:10.1126/science.1065680, 2001.
- 1489 Bosc, E., Bricaud, A., and Antoine, D.: Seasonal and interannual variability in algal
 1490 biomass and primary production in the Mediterranean Sea, as derived from 4 years
 1491 of SeaWiFS observations, *Global Biogeochem. Cy.*, 18, 2003–2034,
 1492 doi:10.1029/2003GB002034, 2004.
- 1493 Boyle, E. A.: Manganese carbonate overgrowths on foraminifera tests, *Geochim.*
 1494 *Cosmochim. Ac.*, 47, 1815–1819, 1983.
- 1495 [Budillon F., Lirer F., Iorio M., Macri P., Sagnotti L., Vallefucio M., Ferraro L., Innangi](#)
 1496 [S., Sahabi M., Tonielli R.: Integrated stratigraphic reconstruction for the last 80 kyr](#)
 1497 [in a deep sector of the Sardinia Channel \(Western Mediterranean\), *Deep Sea Res*](#)
 1498 [Part II Top Stud. Oceanogr., 56, 725–737, 2009.](#)
- 1499 Büntgen, U., Tegel, W., Nicolussi, K., McCormick, M., Frank, D., Trouet, V., Kaplan,
 1500 J. O., Herzig, F., Heussner, K. U., Wanner, H., Luterbacher, J., and Esper, J.: 2500
 1501 years of European climate variability and human susceptibility, *Science*, 331, 578–
 1502 82, doi:10.1126/science.1197175, 2011.
- 1503 Cacho, I., Pelejero, C., Grimalt, J. O., Calafat, A., and Canals, M.: C37 alkenone
 1504 measurements of sea surface temperature in the Gulf of Lions (NW Mediterranean),
 1505 *Org. Geochem.*, 30, 557–566, 1999a.
- 1506 Cacho, I., Grimalt, J. O., Pelejero, C., Canals, M., Sierro, F. J., Flores, J. A., and
 1507 Shackleton, N.: Dansgaard-Oeschger and Heinrich event imprints in Alboran Sea
 1508 paleotemperatures, *Paleoceanography*, 14, 698–705, 1999b.
- 1509 Cacho, I., Grimalt, J. O., Sierro, F. J., Shackleton, N., and Canals, M.: Evidence for
 1510 enhanced Mediterranean thermohaline circulation during rapid climatic coolings,
 1511 *Earth Planet. Sc. Lett.*, 183, 417–429, doi:10.1016/S0012-821X(00)00296-X, 2000.
- 1512 Cacho, I., Grimalt, J., Canals, M., Sbaffi, L., Shackleton, N. J., Schönfeld, J., and Zahn,
 1513 R.: Variability of the western Mediterranean Sea surface temperature during the last
 1514 25,000 years and its connection with the Northern Hemisphere climatic changes,
 1515 *Paleoceanography*, 16, 40–52, 2001.
- 1516 [Cacho, I., Shackleton, N., Elderfield, H., Sierro, F. J. and Grimalt, J. O.: Glacial rapid](#)
 1517 [variability in deep-water temperature and \$\delta^{18}\text{O}\$ from the Western Mediterranean Sea,](#)
 1518 [*Quat. Sci. Rev.*, 25, 3294–3311, doi:10.1016/j.quascirev.2006.10.004, 2006.](#)
- 1519 Calafat, A. M., Casamor, J., Canals, M., and Ny_eler, F.: Distribución y composición
 1520 elemental de la materia particulada en suspensión en el Mar Catalano-Balear,
 1521 *Geogaceta*, 20, 370–373, 1996.
- 1522 Calvert, S. and Pedersen, T.: Sedimentary geochemistry of manganese: implications for
 1523 the environment of formation of manganiferous black shales, *Econ. Geol.*, 91, 36–
 1524 47, 1996.
- 1525 Canals, M., Puig, P., Madron, X. D. De, Heussner, S., Palanques, A., and Fabres, J.:
 1526 Flushing submarine canyons, *Nature*, 444, 354–357, doi:10.1038/nature05271,
 1527 2006.
- 1528 Chen, L., Zonneveld, K. A. F., and Versteegh, G. J. M.: The Holocene Paleoclimate of
 1529 the Southern Adriatic Sea region during the “Medieval Climate Anomaly” reflected
 1530 by organic walled dinoflagellate cysts, *The Holocene*, 23, 645–655,
 1531 doi:10.1177/0959683612467482, 2013.
- 1532 Cléroux, C., Cortijo, E., Anand, P., Labeyrie, L., Bassinot, F., Caillon, N., and
 1533 Duplessy, J. C.: Mg/Ca and Sr/Ca ratios in planktonic foraminifera: proxies for
 1534 upper water column temperature reconstruction, *Paleoceanography*, 23, PA3214,

- 1535 doi:10.1029/2007PA001505, 2008.
- 1536 Combourieu Nebout, N., Turon, J., Zahn, R., Capotondi, L., Londeix, L., and Pahnke,
1537 K.: Enhanced aridity and atmospheric high-pressure stability over the western
1538 Mediterranean during the North Atlantic cold events of the past 50 k.y., *Geology*,
1539 30, 863–866, 2002.
- 1540 Combourieu Nebout, N., Peyron, O., Dormoy, I., Desprat, S., Beaudouin, C., Kotthoff,
1541 U., and Marret, F.: 5 Rapid climatic variability in the west Mediterranean during the
1542 last 25 000 years from high resolution pollen data, *Clim. Past*, 5, 503–521,
1543 doi:10.5194/cp-5-503-2009, 2009.
- 1544 Conte, M. H., Sicre, M. A., Rühlemann, C., Weber, J. C., Schulte, S., Schulz-Bull, D.,
1545 and Blanz, T.: Global temperature calibration of the alkenone unsaturation index
1546 ($U^{K'_{37}}$) in surface waters and comparison with surface sediments, *Geochem.*
1547 *Geophys. Geosy.*, 7, 2, doi:10.1029/2005GC001054, 2006.
- 1548 Coplen, T.: New guidelines for reporting stable hydrogen, carbon, and oxygen isotope-
1549 ratio data, *Geochim. Cosmochim. Ac.*, 60, 3359–3360, 1996.
- 1550 Corella, J. P., Moreno, A., Morellón, M., Rull, V., Giral, S., Rico, M. T., Pérez-Sanz,
1551 A., and Valero-Garcés, B. L.: Climate and human impact on a meromictic lake
1552 during the last 6000 years (Montcortés Lake, Central Pyrenees, Spain), *J.*
1553 *Palaeolimnol.*, 46, 351–367, 2011.
- 1554 Craig, H.: The measurement of oxygen isotope paleotemperatures, in: *Stable Isotopes in*
1555 *Oceanographic Studies and Paleotemperatures*, edited by: Tongiorgi, E., Consiglio
1556 Nazionale delle Ricerche, Laboratorio di Geologia Nucleare, Pisa, 1–24, 1965.
- 1557 D'Ortenzio, F. and Ribera d'Alcalà, M.: On the trophic regimes of the Mediterranean
1558 Sea: a satellite analysis, *Biogeosciences*, 6, 139–148, doi:10.5194/bg-6-139-2009,
1559 2009.
- 1560 Dahl-Jensen, D., Mosegaard, K., Gundestrup, N., Clow, G. D., Johnsen, S. J., Hansen,
1561 A. W., and Balling, N.: Past temperatures directly from the Greenland ice sheet,
1562 *Science*, 282, 268–271, 1998.
- 1563 Demirov, E. and Pinardi, N.: Simulation of the Mediterranean Sea circulation from
1564 1979 to 1993: Part I. The interannual variability, *J. Marine Syst.*, 33–34, 23–50,
1565 2002.
- 1566 Di Bella, L., Frezza, V., Bergamin, L., Carboni, M. G., Falese, F., Mortorelli, E.,
1567 Tarragoni, C., and Chiocci, F. L.: Foraminiferal record and high-resolution seismic
1568 stratigraphy of the Late **Holocene** succession of the submerged Ombrone River delta
1569 (Northern Tyrrhenian Sea, Italy), *Quatern. Int.*, 328–329, 287–300, 2014.
- 1570 Eglinton, T. I., Conte, M. H., Eglinton, G., and Hayes, J. M.: Proceedings of a
1571 workshop on alkenone-based paleoceanographic indicators, *Geochem. Geophys.*
1572 *Geosy.*, 2, 1, doi:10.1029/2000GC000122, 2001.
- 1573 Elderfield, H. and Ganssen, G.: Past temperature and $\delta^{18}\text{O}$ of surface ocean waters
1574 inferred from foraminiferal Mg/Ca ratios, *Nature*, 405, 442–445, 2000.
- 1575 Esper, J., Frank, D. C., Buntgen, U., Verstege, A., Luterbacher, J., and Xoplaki, E.:
1576 Long-term drought severity variations in Morocco, *Geophys. Res. Lett.*, 34, L17702,
1577 doi:10.1029/2007GL030844, 2007.
- 1578 Esper, J., Duthorn, E., Krusic, P. J., Timonen, M., and Buntgen, U.: Northern European
1579 summer temperature variations over the Common Era from integrated tree-ring
1580 density records, *J. Quat. Sci.*, 29, 487–494, doi:10.1002/jqs.2726, 2014.
- 1581 Estrada, M., Vives, F., and Alcaraz, M.: Life and productivity in the open sea, in:
1582 *Western Mediterranean*, edited by: Margalef, R., Oxford, Pergamon Press, 148–197,
1583 1985.
- 1584 Fanget, A. S., Bassetti, M. A., Arnaud, M., Choleau, J. F., Cossa, D., Goineau,

- 1585 A., Fontanier, C., Buscail, R., Jouet, G., Maillet, G. M., Negri, A., Dennielou, B.,
 1586 and Berné, S.: Historical evolution and extreme climate events during the last 400
 1587 years on the Rhone prodelta (NW Mediterranean), *Mar. Geol.*, 346, 375–391,
 1588 doi:10.1016/j.margeo.2012.02.007, 2013.
- 1589 Ferguson, J. E., Henderson, G. M., Kucera, M., and Rickaby, R. E. M.: Systematic
 1590 change of foraminiferal Mg/Ca ratios across a strong salinity gradient, *Earth Planet.*
 1591 *Sc. Lett.*, 265, 153–166, doi:10.1016/j.epsl.2007.10.011, 2008.
- 1592 Fleitmann, D., Cheng, H., Badertscher, S., Edwards, R. L., Mudelsee, M., G. Türk, O.
 1593 M., Fankhauser, A., Pickering, R., Raible, C. C., Matter, A., Kramers, J., and
 1594 Tüysüz, O.: Timing and climatic impact of Greenland interstadials recorded in
 1595 stalagmites from northern Turkey, *Geophys. Res. Lett.*, 36, L19707,
 1596 doi:10.1029/2009GL040050, 2009.
- 1597 Fletcher, W. J. and Sánchez Goñi, M. F.: Orbital and sub-orbital-scale climate impacts
 1598 on vegetation of the western Mediterranean basin over the last 48 000 yr, *Quaternary*
 1599 *Res.*, 70, 451–464, 2008.
- 1600 Fletcher, W. J., Debret, M., and Sanchez Goñi, M.: Mid-Holocene emergence of a low-
 1601 frequency millennial oscillation in western Mediterranean climate: implications for
 1602 past dynamics of the North Atlantic atmospheric westerlies, *The Holocene*, 23, 153–
 1603 166, doi:10.1177/0959683612460783, 2012.
- 1604 Frigola, J.: Variabilitat climàtica ràpida a la conca occidental del Mediterrani: registre
 1605 sedimentològic, Ph.D. Thesis, Dept. of Stratigraphy, Paleontology and Marine
 1606 Geosciences, University of Barcelona, Spain, 2012.
- 1607 Frigola, J., Moreno, A., Cacho, I., Canals, M., Sierro, F. J., Flores, J. A., Grimalt, J. O.,
 1608 Hodell, D. A., and Curtis, J. H.: Holocene climate variability in the western
 1609 Mediterranean region from a deepwater sediment record, *Paleoceanography*, 22,
 1610 PA2209, doi:10.1029/2006PA001307, 2007.
- 1611 Frigola, J., Moreno, A., Cacho, I., Canals, M., Sierro, F. J., Flores, J. A., and Grimalt,
 1612 J. O.: Evidence of abrupt changes in Western Mediterranean Deep Water circulation
 1613 during the last 50 kyr: a high-resolution marine record from the Balearic Sea,
 1614 *Quatern. Int.*, 181, 88–104, doi:10.1016/j.quaint.2007.06.016, 2008.
- 1615 Frisia, S., Borsato, A., Preto, N., and McDermott, F.: Late Holocene annual growth in
 1616 three Alpine stalagmites records the influence of solar activity and the North
 1617 Atlantic Oscillation on winter climate, *Earth Planet. Sci. Lett.*, 216, 411–424, 2003.
- 1618 Ganssen, G. M. and Kroon, D.: The isotopic signature of planktonic foraminifera from
 1619 NE Atlantic surface sediments: implications for the reconstruction of past oceanic
 1620 conditions, *J. Geol. Soc. London*, 157, 693–699, 2000.
- 1621 [Gao, C., Robock, A. and Ammann, C.: Volcanic forcing of climate over the past 1500](#)
 1622 [years: An improved ice core-based index for climate models, *J. Geophys. Res.*, 113,](#)
 1623 [D23111, doi:10.1029/2008JD010239, 2008.](#)
- 1624 Garcia-Orellana, J., Pates, J. M., Masqué, P., Bruach, J. M., and Sanchez-Cabeza, J. A.:
 1625 Distribution of artificial radionuclides in deep sediments of the Mediterranean Sea,
 1626 *Sci. Total Environ.*, 407, 887–98, doi:10.1016/j.scitotenv.2008.09.018, 2009. Giorgi,
 1627 F.: Climate change hot-spots, *Geophys. Res. Lett.*, 33, L08707,
 1628 doi:10.1029/2006GL025734, 2006.
- 1629 Goudeau, M. L. S., Reichert, G. J., Wit, J. C., de Nooijer, L. J., Grauel, A. L.,
 1630 Bernasconi, S. M., and de Lange, G. J.: Seasonality variations in the Central
 1631 Mediterranean during climate change events in the Late Holocene, *Palaeogeogr.*
 1632 *Palaeoclimatol.*, 418, 304–318, 2015.
- 1633 Goy, J. L., Zazo, C., and Dabrio, C. J.: A beach-ridge progradation complex reflecting
 1634 periodical sea-level and climate variability during the Holocene (Gulf of Almeria,

- 1635 Western Mediterranean), *Geomorphology*, 50, 251–268, 2003.
- 1636 Gray, S. T., Graumlich, L. J., Betancourt, J. L., and Pederson, G. T.: A tree-ring based
1637 reconstruction of the Atlantic Multidecadal Oscillation since 1567 A. D., *Geophys.*
1638 *Res. Lett.*, 31,12, doi:10.1029/2004GL019932, 2004.
- 1639 Griggs, C., DeGaetano, A., Kuniholm, P., and Newton, M.: A regional high-frequency
1640 reconstruction of May–June precipitation in the north Aegean from oak tree rings,
1641 AD 1089–1989, *Int. J. Climatol.*, 27, 1075–1089, 2007.
- 1642 Grauel, A. L., Goudeau, M. L. S., de Lange, G. J., and Bernasconi, S. M.: Climate of
1643 the past 2500 years in the Gulf of Taranto, central Mediterranean Sea: a high-
1644 resolution climate reconstruction based on $\delta^{18}\text{O}$ and $\delta^{13}\text{C}$ of *Globigerinoides ruber*
1645 (white), *The Holocene*, 23,1440–1446, doi:10.1177/0959683613493937, 2013.
- 1646 Guemas, V., García-Serrano, J., Mariotti, A., Doblás-Reyes, F., and Caron, L. P.:
1647 Prospects for decadal climate prediction in the Mediterranean region, *Q. J. Roy.*
1648 *Meteor. Soc.*, 141, 580–597, doi:10.1002/qj.2379, 2014.
- 1649 Hernández-Almeida, I., Bárcena, M. Á., Flores, J. A., Sierro, F. J., Sánchez-Vidal, A.,
1650 and Calafat, A.: Microplankton response to environmental conditions in the Alboran
1651 Sea (Western Mediterranean): one year sediment trap record, *Mar. Micropaleontol.*,
1652 78, 14–24, doi:10.1016/j.marmicro.2010.09.005, 2011.
- 1653 Holzhauser, H., Magny, M., and Heinz, J.: Glacier and lake-level variations in west-
1654 central Europe over the last 3500 years, *The Holocene*, 15, 789–801, 2005.
- 1655 Hönisch, B., Allen, K. A., Lea, D. W., Spero, H. J., Eggins, S. M., Arbuszewski, J.,
1656 DeMenocal, P., Rosenthal, Y., Russell, A. D., and Elderfield, H.: The influence of
1657 salinity on Mg/Ca in planktic foraminifers – evidence from cultures, core-top
1658 sediments and complementary $\delta^{18}\text{O}$, *Geochim. Cosmochim. Ac.*,121, 196–213,
1659 2013.
- 1660 Hoogakker, B. A. A., Klinkhammer, G. P., Elderfield, H., Rohling, E. J., and Hayward,
1661 C.: Mg/Ca paleothermometry in high salinity environments, *Earth Planet. Sc. Lett.*,
1662 284, 583–589, doi:10.1016/j.epsl.2009.05.027, 2009.
- 1663 Huang, S.: Merging information from different resources for new insights into climate
1664 change in the past and future, *Geophys. Res. Lett.*, 31, 1–4,
1665 doi:10.1029/2004GL019781, 2004.
- 1666 Hughes, M. K. and Diaz, H. F.: Was there a “Medieval warm period”, and if so, where
1667 and when?, *Clim. Change*, 109–142, 1994.
- 1668 Hurrell, J. W.: Decadal Trends in the North Atlantic Oscillation: regional temperatures
1669 and precipitation, *Science*, 269, 676–679, doi:10.1126/science.269.5224.676, 1995.
- 1670 Incarbona, A., Ziveri, P., Di Stefano, E., Lirer, F., Mortyn, G., Patti, B., Pelosi, N.,
1671 Sprovieri, M., Tranchida, G., Vallefucio, M., Albertazzi, S., Bellucci, L. G.,
1672 Bonanno, A., Bonomo, S., Censi, P., Ferraro, L., Giuliani, S., Mazzola, S., and
1673 Sprovieri, R.: The Impact of the Little Ice Age on Coccolithophores in the Central
1674 Mediterranean Sea, *Clim. Past*, 6, 795–805, doi:10.5194/cp-6-795-2010, 2010.
- 1675 Jalut, G., Esteban Amat, A., Mora, S. R., Fontugne, M., Mook, R., Bonnet, L., and
1676 Gauquelin, T.: Holocene climatic changes in the western Mediterranean: installation
1677 of the Mediterranean climate, *CR. Acad. Sci. Ser. II*, 325, 327–334, 1997.
- 1678 Jalut, G., Esteban Amat, A., Bonnet, L., Gauquelin, T., and Fontugne, M.: Holocene
1679 climatic changes in the Western Mediterranean, from south-east France to south-east
1680 Spain, *Palaeogeogr. Palaeoclimatol.*, 160, 255–290, 2000.
- 1681 Joerin, U. E., Stocker, T. F., Schlu, C., and Physics, E.: Multicentury glacier
1682 fluctuations in the Swiss Alps during the Holocene, *The Holocene*, 16, 697–704,
1683 2006.
- 1684 Kaufman, D. S., Schneider, D. P., McKay, N. P., Ammann, C. M., Bradley, R. S., Bri_

1685 a, K. R., Miller, G. H., Otto-Bliesner, B. L., Overpeck, J. P., and Vinther, B. M.:
1686 Recent warming reverses long-term arctic cooling, *Science*, 325, 1236–1239,
1687 doi:10.1126/science.1173983, 2009.

1688 Kobashi, T., Kawamura, K., Severinghaus, J. P., Barnola, J. M., Nakaegawa, T.,
1689 Vinther, B. M., Johnsen, S. J., and Box, J. E.: High variability of Greenland surface
1690 temperature over the past 4000 years estimated from trapped air in an ice core,
1691 *Geophys. Res. Lett.*, 38, 21, doi:10.1029/2011GL049444, 2011.

1692 Krishnaswami, S., Lal, D., Martin, J. M., and Meybeck, M.: Geochronology of lake
1693 sediments, *Earth. Planet. Sci. Lett.*, 11, 407–414, 1971.

1694 Labuhn, I., Genty, D., Vonhof, H., Bourdin, C., Blamart, D., Douville, E., Ruan, J.,
1695 Cheng, H., Edwards, R. L., Pons-Branchu, E., and Pierre, M.: A high-resolution
1696 fluid inclusion $\delta^{18}\text{O}$ record from a stalagmite in SW France: modern calibration and
1697 comparison with multiple proxies, *Quaternary Sci. Rev.*, 110, 152–165,
1698 doi:10.1016/j.quascirev.2014.12.021, 2015.

1699 Lacombe, H., Gascard, J. C., Cornella, J., and Béthoux, J. P.: Response of the
1700 Mediterranean to the water and energy fluxes across its surface, on seasonal and
1701 interannual scales, *Oceanol. Acta*, 4, 247–255, 1981.

1702 Lacombe, H., Tchernia, P., and Gamberoni, L.: Variable bottom water in the Western
1703 Mediterranean basin, *Prog. Oceanogr.*, 14, 319–338, 1985.

1704 Larsen, L. B., Vinther, B. M., Bri_ a, K. R., Melvin, T. M., Clausen, H. B., Jones, P. D.,
1705 Siggaard-Andersen, M. L., Hammer, C. U., Eronen, M., Grudd, H., Gunnarson, B.
1706 E., Hantemirov, R. M., Naurzbaev, M. M., and Nicolussi, K.: New ice core evidence
1707 for a volcanic cause of the A.D. 536 dust veil, *Geophys. Res. Lett.*, 35, 1–5,
1708 doi:10.1029/2007GL032450, 2008.

1709 Laskar, J., Robutel, P., Joutel, F., Gastineau, M., Correia, A. C. M., and Levrard, B.: A
1710 longterm numerical solution for the insolation quantities of the Earth, *Astron.*
1711 *Astrophys.*, 285, 261–285, 2004.

1712 Lea, D. W., Mashiotta, T. A., and Spero, H. J.: Controls on magnesium and strontium
1713 uptake in planktonic foraminifera determined by live culturing, *Geochim.*
1714 *Cosmochim. Ac.*, 63, 2369–2379, 1999.

1715 Lea, D. W., Pak, D. K., and Paradis, G.: Influence of volcanic shards on foraminiferal
1716 Mg/Ca in a core from the Galápagos region, *Geochem. Geophys. Geosy.*, 6, 11,
1717 doi:10.1029/2005GC000970, 2005.

1718 Lebreiro, S. M., Francés, G., Abrantes, F. F. G., Diz, P., Bartels-Jónsdóttir, H. B.,
1719 Stroynowski, Z. N., Gil, I. M., Pena, L. D., Rodrigues, T., Jones, P. D., Nombela, M.
1720 A., Alejo, I., Bri_ a, K. R., Harris, I., and Grimalt, J. O.: Climate change and coastal
1721 hydrographic response along the Atlantic Iberian margin (Tagus Prodelta and Muros
1722 Ría) during the last two millennia, *The Holocene*, 16, 1003–1015, 2006.

1723 Lehner, F., Raible, C. C., and Stocker, T. F.: Testing the robustness of a precipitation
1724 proxy-based North Atlantic Oscillation reconstruction, *Quaternary Sci. Rev.*, 45,
1725 85–94, doi:10.1016/j.quascirev.2012.04.025, 2012.

1726 Lionello, P.: *The Climate of the Mediterranean Region: From the Past to the Future*,
1727 Elsevier Science, Burlington, MA, 2012.

1728 Lionello, P. and Sanna, A.: Mediterranean wave climate variability and its links with
1729 NAO and Indian Monsoon, *Clim. Dynam.*, 25, 611–623, doi:10.1007/s00382-005-
1730 0025-4, 2005.

1731 Lionello, P., Malanott-Rizzoli, R., Boscolo, R., Alpert, P., Artale, V., Li, L.,
1732 Luterbacher, J., May, W., Trigo, R., Tsimplis, M., Ulbrich, U., and Xoplaki, E.: The
1733 Mediterranean climate: An overview of the main characteristics and issues, in:
1734 *Mediterranean Climate Variability (MedClivar)*, Elsevier, Amsterdam, 1–26, 2006.

- 1735 Lirer, F., Sprovieri, M., Ferraro, L., Vallefucio, M., Capotondi, L., Cascella, A.,
1736 Petrosino, P., Insinga, D. D., Pelosi, N., Tamburrino, S., and Lubritto, C.: Integrated
1737 stratigraphy for the Late Quaternary in the eastern Tyrrhenian Sea, *Quatern. Int.*,
1738 292, 71–85, doi:10.1016/j.quaint.2012.08.2055, 2013.
- 1739 Lirer, F., Sprovieri, M., Vallefucio, M., Ferraro, L., Pelosi, N., Giordano, L., and
1740 Capotondi, L.: Planktonic foraminifera as bio-indicators for monitoring the climatic
1741 changes that have occurred over the past 2000 years in the southeastern Tyrrhenian
1742 Sea, *Integr. Zool.*, 9, 542–54, doi:10.1111/1749-4877.12083, 2014.
- 1743 Luterbacher, J., Dietrich, D., Xoplaki, E., Grosjean, M., and Wanner, H.: European
1744 seasonal and annual temperature variability, trends, and extremes since 1500,
1745 *Science*, 303, 1499–1503, doi:10.1126/science.1093877, 2004.
- 1746 Malanotte-Rizzoli, P., Artale, V., Borzelli-Eusebi, G. L., Brenner, S., Crise, A., Gacic,
1747 M., Kress, N., Marullo, S., Ribera d'Alcalà, M., Sofianos, S., Tanhua, T.,
1748 Theocharis, A., Alvarez, M., Ashkenazy, Y., Bergamasco, A., Cardin, V., Carniel,
1749 S., Civitarese, G., D'Ortenzio, F., Font, J., Garcia-Ladona, E., Garcia-Lafuente, J.
1750 M., Gogou, A., Gregoire, M., Hainbucher, D., Kontoyannis, H., Kovacevic, V.,
1751 Kraskapoulou, E., Kroskos, G., Incarbona, A., Mazzocchi, M. G., Orlic, M., Ozsoy,
1752 E., Pascual, A., Poulain, P.-M., Roether, W., Rubino, A., Schroeder, K., Siokou-
1753 Frangou, J., Souvermezoglou, E., Sprovieri, M., Tintoré, J., and Triantafyllou, G.:
1754 Physical forcing and physical/biochemical variability of the Mediterranean Sea: a
1755 review of unresolved issues and directions for future research, *Ocean Sci.*, 10, 281–
1756 322, doi:10.5194/os-10-281-2014, 2014.
- 1757 Maldonado, A., Got, H., Monaco, A., O'Connell, S., and Mirabile, L.: Valencia Fan
1758 (northwestern Mediterranean): distal deposition fan variant, *Mar. Geol.*, 62, 295–
1759 319, 1985.
- 1760 Mangini, A., Spötl, C., and Verdes, P.: Reconstruction of temperature in the Central
1761 Alps during the past 2000 yr from a $\delta^{18}\text{O}$ stalagmite record, *Earth. Planet. Sci. Lett.*,
1762 235, 741–751, 2005.
- 1763 Mann, M. E., Zhang, Z., Hughes, M. K., Bradley, R. S., Miller, S. K., Rutherford, S.,
1764 and Ni, F.: Proxy-based reconstructions of hemispheric and global surface
1765 temperature variations over the past two millennia, *P. Natl. Acad. Sci. USA*, 105,
1766 13252–13257, 2008.
- 1767 Mann, M. E., Zhang, Z., Rutherford, S., Bradley, R. S., Hughes, M. K., Shindell, D.,
1768 Ammann, C., Faluvegi, G., and Ni, F.: Global signatures and dynamical origins of
1769 the little ice age and medieval climate anomaly, *Science*, 326, 1256–1260, 2009.
- 1770 Marchal, O., Cacho, I., Stocker, T. F., Grimalt, J. O., Calvo, E., Martrat, B., Shackleton,
1771 N., Vautravers, M., Cortijo, E., Van Kreveld, S., Andersson, C., Ko, N., Chapman,
1772 M., Sbaiffi, L., Duplessy, J., Sarnthein, M., and Turon, J.: Apparent long-term
1773 cooling of the sea surface in the northeast Atlantic and Mediterranean during the
1774 Holocene, *Quaternary Sci. Rev.*, 21, 455–483, 2002.
- 1775 [Margaritelli G., Lirer F., Vallefucio M., Bonomo S., Cascella A., Capotondi L., Ferraro](#)
1776 [L., Insinga D.D., Petrosino P., Rettori R.: Climatic variability during the last two](#)
1777 [millennia in the Tyrrhenian Sea: evidences from planktonic foraminifera and](#)
1778 [geochemical data, XV Edizione delle “Giornate di Paleontologia”](#)
1779 [PALEODAYS2015, Palermo 17-29 Maggio 2015, 72-73. Società Paleontologica](#)
1780 [Italiana, 2015.](#)
- 1781 Mariotti, A.: Decadal climate variability and change in the Mediterranean Region, *Sci.*
1782 *Technol. Infus. Clim. Bull.*, Climate Test Bed Joint Seminar Series, Maryland, US
1783 National Oceanic and Atmospheric Administration, 1–5, 2011.
- 1784 Martin, J., Elbaz-Poulichet, F., Guieu, C., Lo, e-Pilot, M., and Han, G.: River versus

- 1785 atmospheric input of material to the Mediterranean Sea: an Overview, *Mar. Chem.*,
1786 28, 159–182, 1989.
- 1787 Martín-Chivelet, J., Muñoz-García, M. B., Edwards, R. L., Turrero, M. J., and Ortega,
1788 A. I.: Land surface temperature changes in Northern Iberia since 4000 yr BP, based
1789 on $\delta^{13}\text{C}$ of speleothems, *Glob. Planet. Change.*, 77, 1–12,
1790 doi:10.1016/j.gloplacha.2011.02.002, 2011.
- 1791 Martín-Puertas, C., Valero-Garcés, B. L., Brauer, A., Mata, M. P., Delgado-Huertas, A.,
1792 and Dulski, P.: The Iberian–Roman Humid Period (2600–1600 cal yr BP) in the
1793 Zoñar Lake varve record (Andalucía, Southern Spain), *Quaternary Res.*, 71, 2,
1794 doi:10.1016/j.yqres.2008.10.004, 2008.
- 1795 Martínez-Cortizas, A., Pontevedra-Pombal, X., García-Rodeja, E., Nóvoa-Muñoz, J. C.,
1796 and Shotyk, W.: Mercury in a Spanish Peat Bog: archive of climate change and
1797 atmospheric metal deposition, *Science*, 284, 939–942, 1999.
- 1798 Martrat, B., Grimalt, J. O., Lopez-Martinez, C., Cacho, I., Sierro, F. J., Flores, J. A.,
1799 Zahn, R., Canals, M., Curtis, J. H., and Hodell, D. A.: Abrupt temperature changes
1800 in the Western Mediterranean over the past 250 000 years, *Science*, 306, 1762,
1801 doi:10.1126/science.1101706, 2004.
- 1802 Marullo, S., Artale, V., and Santoleri, R.: The SST multi-decadal variability in the
1803 Atlantic-Mediterranean region and its relation to AMO, *J. Climate*, 24, 4385–4401,
1804 doi:10.1175/2011JCLI3884.1, 2011.
- 1805 Mashiotta, T. A., Lea, D. W., and Spero, H. J.: Glacial–interglacial changes in
1806 Subantarctic sea surface temperature and $\delta^{18}\text{O}$ -water using foraminiferal Mg, *Earth*
1807 *Planet. Sc. Lett.*, 170, 417–432, 1999.
- 1808 Masqué, P., Fabres, J., Canals, M., Sanchez-Cabeza, J. A., Sanchez-Vidal, A., Cacho, I.,
1809 Calafat, A. M., and Bruach, J. M.: Accumulation rates of major constituents of
1810 hemipelagic sediments in the deep Alboran Sea: a centennial perspective of
1811 sedimentary dynamics, *Mar. Geol.*, 193, 207–233, 2003.
- 1812 Matthews, J. A. and Bri_a, K. R.: The “Little ice age”: re-evaluation of an evolving
1813 concept, *Geogr. Ann. A*, 87, 17–36, 2005.
- 1814 Mauffret, A.: Etude géodynamique de la marge des Illes Baléares, *Mémoires de la*
1815 *Société Géologique de France LVI*, 1–96, 1979.
- 1816 Mayewski, P. A., Rohling, E. E., Stager, J. C., Karlen, W., Maasch, K. A., Meeker, L.
1817 D., Meyerson, E. A., Gasse, F., van Kreveld, S., Holmgren, K., Lee-Thorp, J.,
1818 Rosqvist, G. Rack, F., Staubwasser, M., Schneider, R. R., and Steig, E. J.: Holocene
1819 climate variability, *Quaternary Res.*, 62, 243–255, 2004.
- 1820 McConnell, M. C. and Thunell, R. C.: Calibration of the planktonic foraminiferal
1821 Mg/Ca paleothermometer: sediment trap results from the Guaymas Basin, Gulf of
1822 California, *Paleoceanography*, 20, PA2016, doi:10.1029/2004PA001077, 2005.
- 1823 [McGregor, H. V., Evans, M. N., Goosse, H., Leduc, G., Martrat, B., Addison, J. A.,](#)
1824 [Graham Mortyn, P., Oppo, D. W., Seidenkrantz, M.-S., Sicre, M.-A., Phipps, S. J.,](#)
1825 [Selvaraj, K., Thirumalai, K., Filipsson, H. L. and Ersek, V.: Robust global ocean](#)
1826 [cooling trend for the pre-industrial Common Era, *Nat Geosci*, 8\(9\), 671–677,](#)
1827 [doi:10.1038/ngeo2510, 2015.](#)
- 1828 MEDAR GROUP, MEDATLAS/2002 European Project: Mediterranean and Black Sea
1829 Database of Temperature Salinity and Bio-Chemical Parameters, Climatological
1830 Atlas, Institut Français de Recherche pour L’Exploitation de la Mer (IFREMER),
1831 Edition/Instituto Nazionale di Oceanografia e di Geofisica Sperimentale (OGS),
1832 2002.
- 1833 Medoc, G.: Observation of formation of Deep Water in the Mediterranean Sea, *Nature*,
1834 227, 1037–1040, 1970.

- 1835 Millán, M. M., Estrela, M. J., Sanz, M. J., Mantilla, E., Martín, M., Pastor, F., Salvador,
1836 R., Vallejo, R., Alonso, L., Gangoiti, G., Iardia, J. L., Navazo, M., Albizuri, A.,
1837 Artiñano, B., Ciccioioli, P., Kallos, G., Carvalho, R. A., Andrés, D., Ho_ , A.,
1838 Werhahn, J., Seufert, G., and Versino, B.: Climatic feedbacks and desertification:
1839 the Mediterranean Model, *J. Climate*, 18, 684–701, 2005.
- 1840 Millot, C.: Circulation in the Western Mediterranean Sea, *J. Marine Syst.*, 20, 423–442,
1841 1999.
- 1842 Morellón, M., Pérez-Sanz, A., Corella, J. P., Büntgen, U., Catalán, J., González-
1843 Sampériz, P., González-Trueba, J. J., López-Sáez, J. A., Moreno, A., Pla-Rabes, S.,
1844 Saz-Sánchez, M. Á., Scussolini, P., Serrano, E., Steinhilber, F., Stefanova, V.,
1845 Vegas-Vilarrúbia, T., and Valero-Garcés, B.: A multi-proxy perspective on
1846 millennium-long climate variability in the Southern Pyrenees, *Clim. Past*, 8, 683–
1847 700, doi:10.5194/cp-8-683-2012, 2012.
- 1848 Moreno, A., Cacho, I., Canals, M., Prins, M. A., Sánchez-Goñi, M. F., Grimalt, J. O.,
1849 and Weltje, G. J.: Saharan Dust Transport and High-Latitude Glacial Climatic
1850 Variability: the Alboran Sea Record, *Quaternary Res.*, 58, 318–328,
1851 doi:10.1006/qres.2002.2383, 2002.
- 1852 Moreno, A., Cacho, I., Canals, M., Grimalt, J. O., Sánchez-Goñi, M. F., Shackleton, N.,
1853 and Sierro, F. J.: Links between marine and atmospheric processes oscillating on a
1854 millennial time-scale. A multi-proxy study of the last 50,000 yr from the Alboran
1855 Sea (Western Mediterranean Sea), *Quaternary Sci. Rev.*, 24, 1623–1636,
1856 doi:10.1016/j.quascirev.2004.06.018, 2005.
- 1857 Moreno, A., Valero-Garcés, B. L., González-Sampériz, P., and Rico, M.: Flood
1858 response to rainfall variability during the last 2000 years inferred from the Taravilla
1859 Lake record (Central Iberian Range, Spain), *J. Paleolimnol.*, 40, 943–961,
1860 doi:10.1007/s10933-008-9209-3, 2008.
- 1861 Moreno, A., Pérez, A., Frigola, J., Nieto-Moreno, V., Rodrigo-Gámiz, M., Martrat, B.,
1862 González-Sampériz, P., Morellón, M., Martín-Puertas, C., Pablo, J., Belmonte, Á.,
1863 Sancho, C., Cacho, I., Herrera, G., Canals, M., Grimalt, J. O., Jiménez-Espejo, F.,
1864 Martínez-Ruiz, F., Vegas-Vilarrúbia, T., and Valero-Garcés, B. L.: The Medieval
1865 Climate Anomaly in the Iberian Peninsula reconstructed from marine and lake
1866 records, *Quaternary Sci. Rev.*, 43, 16–32, doi:10.1016/j.quascirev.2012.04.007,
1867 2012.
- 1868 Morhange, C., Marriner, N., Excoffon, P., Bonnet, S., Flaux, C., Zibrowius, H., Goiran,
1869 J. P., and El Amouri, M.: Relative Sea-Level Changes During Roman Times in the
1870 Northwest Mediterranean: the 1st Century AD. Fish Tank of Forum Julii, Fréjus,
1871 France, *Geoarchaeology*, 28, 363–372, doi:10.1002/gea.21444, 2013.
- 1872 [Mullitza, S., Boltovskoy, D., Donner, B., Meggers, H., Paul, A. and Wefer, G.:](#)
1873 [Temperature: \$\delta\$ 18O relationships of planktonic foraminifera collected from surface](#)
1874 [waters, *Palaeogeogr Palaeoclimatol Palaeoecol*, 202\(1-2\), 143–152,](#)
1875 [doi:10.1016/S0031-0182\(03\)00633-3, 2003.](#)
- 1876 Nieto-Moreno, V., Martínez-Ruiz, F., Giral, S., Jiménez-Espejo, F., Gallego-Torres,
1877 D., Rodrigo-Gámiz, M., García-Orellana, J., Ortega-Huertas, M., and de Lange, G.
1878 J.: Tracking climate variability in the western Mediterranean during the Late
1879 Holocene: a multiproxy approach, *Clim. Past*, 7, 1395–1414, doi:10.5194/cp-7-
1880 1395-2011, 2011.
- 1881 Nieto-Moreno, V., Martínez-Ruiz, F., Willmott, V., García-Orellana, J., and Masqué,
1882 P.: Organic geochemistry climate conditions in the westernmost Mediterranean over
1883 the last two millennia: an integrated biomarker approach, *Org. Geochem.*, 55, 1–10,
1884 doi:10.1016/j.orggeochem.2012.11.001, 2013.

- 1885 Olsen, J., Anderson, N. J., and Knudsen, M. F.: Variability of the North Atlantic
1886 Oscillation over the past 5200 years, *Nat. Geosci.*, 5, 808–812,
1887 doi:10.1038/ngeo1589, 2012.
- 1888 Ortega, P., Lehner, F., Swingedouw, D., Masson-Delmotte, V., Raible, C. C., Casado,
1889 M., and Yiou, P.: A model-tested North Atlantic Oscillation reconstruction for the
1890 past millennium, *Nature*, 523, 7558, doi:10.1038/nature14518, 2015.
- 1891 PAGES: Science Plan and Implementation Strategy, IGBP Report No. 57, IGBP
1892 Secretariat, Stockholm, 2009.
- 1893 PAGES 2K Consortium: Continental-scale temperature variability during the past two
1894 millennia, *Nature*, 6, 339–346, doi:10.1038/NGEO1797, 2013.
- 1895 Pastor, F.: Ciclogénesis intensas en la cuenca occidental del Mediterráneo y temperatura
1896 superficial del mar: modelización y evaluación de las áreas de recarga, PhD Thesis,
1897 Dept. of Astronomy and Meteorology, University of Barcelona, Spain, 2012.
- 1898 Pastor, F., Estrela, M., Peñarrocha, D., and Millán, M.: Torrential rains on the Spanish
1899 Mediterranean Coast: modeling the effects of the sea surface temperature, *J. Appl.*
1900 *Meteorol.*, 40, 1180–1195, 2001.
- 1901 Patton, G. M., Martin, P. A., Voelker, A., and Salgueiro, E.: Multiproxy comparison of
1902 oceanographic temperature during Heinrich Events in the eastern subtropical
1903 Atlantic, *Earth Planet. Sc. Lett.*, 310, 45–58, doi:10.1016/j.epsl.2011.07.028, 2011.
- 1904 Pena, L. D., Calvo, E., Cacho, I., Eggins, S., and Pelejero, C.: Identification and
1905 removal of Mn-Mg-rich contaminant phases on foraminiferal tests: implications for
1906 Mg/Ca past temperature reconstructions, *Geochem. Geophys. Geosy.*, 6, 9,
1907 doi:10.1029/2005GC000930, 2005.
- 1908 Pena, L. D., Cacho, I., Calvo, E., Pelejero, C., Eggins, S., and Sadekov, A.:
1909 Characterization of contaminant phases in foraminifera carbonates by electron
1910 microprobe mapping, *Geochem. Geophys. Geosy.*, 9, 7, doi:10.1029/2008GC002018,
1911 2008.
- 1912 Pierre, C.: The oxygen and carbon isotope distribution in the Mediterranean water
1913 masses, *Mar. Geol.*, 153, 41–55, 1999.
- 1914 Pinardi, N. and Masetti, E.: Variability of the large general circulation of the
1915 Mediterranean Sea from observations and modelling: a review, *Palaeogeogr.*
1916 *Palaeoclimatol.*, 158, 153–173, 2000.
- 1917 Pinot, J. M., López-Jurado, J., and Riera, M.: The CANALES experiment (1996–1998).
1918 Interannual, seasonal, and mesoscale variability of the circulation in the Balearic
1919 Channels, *Prog. Oceanogr.*, 55, 335–370, 2002.
- 1920 Piva, A., Asioli, A., Trincardi, F., Schneider, R. R., and Vigliotti, L.: Late-Holocene
1921 climate variability in the Adriatic Sea (Central Mediterranean), *The Holocene*, 18,
1922 153–167, 2008.
- 1923 Pla, S. and Catalan, J.: Chrysophyte cysts from lake sediments reveal the submillennial
1924 winter/spring climate variability in the northwestern Mediterranean region
1925 throughout the Holocene, *Clim. Dynam.*, 24, 263–278, 2005.
- 1926 Pujol, C. and Vergnaud-Grazzini, C.: Distribution patterns of live planktic foraminifers
1927 as related to regional hydrography and productive systems of the Mediterranean Sea,
1928 *Mar. Micropaleontol.*, 25, 187–217, 1995.
- 1929 Reguera, M. I.: Respuesta del Mediterráneo Occidental a los cambios climáticos
1930 bruscos ocurridos durante el último glacial: estudio de las asociaciones de
1931 foraminíferos, PhD Thesis, Dept. of Geology, University of Salamanca, Spain, 2004.
- 1932 Reimer, P. J., Bard, E., Bayliss, A., Beck, J. W., Blackwell, P. G., Bronk Ramsey, C.,
1933 Buck, C. E., Edwards, R. L., Friedrich, M., Grootes, P. M., Guilderson, T. P.,
1934 Haflidason, H., Hajdas, I., Hatté, C., Heaton, T. J., Ho_mann, D. L., Hogg, A. G.,

- 1935 Hughen, K. A., Kaiser, K. F., Kromer, B., Manning, S. W., Niu, M., Reimer, R. W.,
 1936 Richards, D. A., Scott, M. E., Southon, J. R., Turney, C. S. M., and van der Plicht,
 1937 J.: Intcal13 and Marine13 radiocarbon age calibration curves 0–50 000 years cal BP,
 1938 Radiocarbon, 55, 1869–1887, 2013.
- 1939 Richter, T. O. and van der Gaast, S.: The Avaatech Core Scanner: technical description
 1940 and applications to NE Atlantic sediments, in: New Ways of Looking at Sediment
 1941 Core and Core Data, edited by: Rothwell, R. G., Geological Society Special
 1942 Publication, London, 39–50, 2006.
- 1943 Rigual-Hernández, A. S., Sierro, F. J., Bárcena, M. A., Flores, J. A., and Heussner, S.:
 1944 Seasonal and interannual changes of planktic foraminiferal fluxes in the Gulf of
 1945 Lions (NW Mediterranean) and their implications for paleoceanographic studies:
 1946 two 12-year sediment trap records, Deep-Sea Res. Pt. I, 66, 26–40,
 1947 doi:10.1016/j.dsr.2012.03.011, 2012.
- 1948 Rigual-Hernández, A. S., Bárcena, M. A., Jordan, R. W., Sierro, F. J., Flores, J. A.,
 1949 Meier, K. J., Beaufort, L., and Heussner, S.: Diatom fluxes in the NW
 1950 Mediterranean: evidence from a 12-year sediment trap record and surficial
 1951 sediments, J. Plankton Res., 35, 5, doi:10.1093/plankt/fbt055, 2013.
- 1952 Roberts, N., Moreno, A., Valero-Garcés, B. L., Corella, J. P., Jones, M., Allcock, S.,
 1953 Woodbridge, J., Morellón, M., Luterbacher, J., Xoplaki, E., and Türkeş, M.:
 1954 Palaeolimnological evidence for an east–west climate see-saw in the Mediterranean
 1955 since AD 900, Global Planet. Change, 84–85, 23–34,
 1956 doi:10.1016/j.gloplacha.2011.11.002, 2012.
- 1957 Rodrigo-Gámiz, M., Martínez-Ruiz, S., Rampen, S., Schouten, S., and Sinninghe
 1958 Damsté, J.: Sea surface temperature variations in the western Mediterranean Sea
 1959 over the last 20 kyr: a dual-organic proxy ($U^{k'}_{37}$ and LDI) approach,
 1960 Paleoceanography, 29, 87–98, doi:10.1002/2013PA002466, 2014.
- 1961 Rogerson, M., Rohling, E. J., Weaver, P. P. E., and Murray, J. W.: The Azores Front
 1962 since the Last Glacial Maximum, Earth Planet. Sc. Lett., 222, 779–789,
 1963 doi:10.1016/j.epsl.2004.03.039, 2004.
- 1964 Rohling, E., Hayes, A., De Rijk, S., Kroon, D., Zachariasse, W. J., and Eisma, D.:
 1965 Abrupt cold spells in the northwest Mediterranean, Paleoceanography, 13, 316–322,
 1966 1998.
- 1967 Sabatier, P., Dezileau, L., Colin, C., Briquieu, L., Bouchette, F., Martinez, P., Siani, G.,
 1968 Raynal, O., and Von Grafenstein, U.: 7000 years of paleostorm activity in the NW
 1969 Mediterranean Sea in response to Holocene climate events, Quaternary Res., 77, 1–
 1970 11, doi:10.1016/j.yqres.2011.09.002, 2012.
- 1971 Sáez de Cámara, E., Gangoiti, G., Alonso, L., and Iza, J.: Daily precipitation in
 1972 Northern Iberia: understanding the recent changes after the circulation variability in
 1973 the North Atlantic sector, J. Geophys. Res., 120, 19, doi:10.1002/2015JD023306,
 1974 2015.
- 1975 Sanchez-Cabeza, J., Masqué, P., and Ani-Ragolta, I.: ^{210}Pb and ^{210}Po analysis in
 1976 sediments and soils by microwave acid digestion, J. Radioanal. Nucl. Ch., 227, 19–
 1977 22, 1998.
- 1978 Schiebel, R., Schmuker, B., Alves, M., and Hemleben, C.: Tracking the Recent and Late
 1979 Pleistocene Azores front by the distribution of planktic foraminifers, J. Marine Syst.,
 1980 37, 213–227, 2002.
- 1981 Schilman, B., Bar-Matthews, M., Almogilabin, A., and Luz, B.: Global climate
 1982 instability reflected by Eastern Mediterranean marine records during the late
 1983 Holocene, Palaeogeogr. Palaeoclimatol., 176, 157–176, 2001.
- 1984 Shackleton, N.: Attainment of isotopic equilibrium between ocean water and the

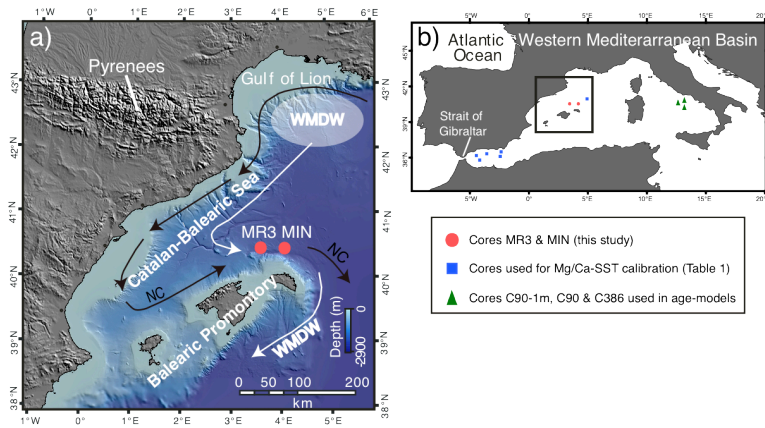
- 1985 benthonic foraminifera genus *Uvigerina*: isotopic changes in the ocean during the
1986 last glacial, CNRS, Colloq. Int., 219, 203–209, 1974.
- 1987 Sicre, A., Ternois, Y., Miquel, J. C., and Marty, J. C.: Alkenones in the Northwestern
1988 Mediterranean sea: interannual variability and vertical transfer, *Geophys. Res. Lett.*,
1989 26, 1735–1738, 1999.
- 1990 Sicre, M. A., Yiou, P., Eiriksson, J., Ezat, U., Guimbaut, E., Dahhaoui, I., Knudsen, K.
1991 L., Jansen, E., and Turon, J. L.: A 4500-year reconstruction of sea surface
1992 temperature variability at decadal time-scales off North Iceland, *Quaternary Sci.*
1993 *Rev.*, 27, 2041–2047, doi:10.1016/j.quascirev.2008.08.009, 2008.
- 1994 Sierro, F. J., Hodell, D. A., Curtis, J. H., Flores, J. A., Reguera, I., Colmenero-Hidalgo,
1995 E., Bárcena, M. A., Grimalt, J. O., Cacho, I., Frigola, J., and Canals, M.: Impact of
1996 iceberg melting on Mediterranean thermohaline circulation during Heinrich events,
1997 *Paleoceanography*, 20, 1–13, doi:10.1029/2004PA001051, 2005.
- 1998 Siokou-Frangou, I., Christaki, U., Mazzocchi, M. G., Montresor, M., Ribera d’Alcalá,
1999 M., Vaqué, D., and Zingone, A.: Plankton in the open Mediterranean Sea: a review,
2000 *Biogeosciences*, 7, 1543–1586, doi:10.5194/bg-7-1543-2010, 2010.
- 2001 Sprovieri, R., Stefano, E. Di, Incarbona, A., and Gargano, M. E.: A high-resolution
2002 record of the last deglaciation in the Sicily Channel based on foraminifera and
2003 calcareous nannofossil quantitative distribution, *Palaeogeogr. Palaeocl.*, 202, 119–
2004 142, doi:10.1016/S0031-0182(03)00632-1, 2003.
- 2005 Steinhilber, F., Beer, J., and Fröhlich, C.: Total solar irradiance during the Holocene,
2006 *Geophys. Res. Lett.*, 36, L19704, doi:10.1029/2009GL040142, 2009.
- 2007 Steinhilber, F., Abreu, J. A., Beer, J., Brunner, I., Christl, M., Fischer, H., Heikkilä, U.,
2008 Kubik, P. W., Mann, M., McCracken, K. G., Miller, H., Miyahara, H., Oerter, H.,
2009 and Wilhelms, F.: 9400 years of cosmic radiation and solar activity from ice cores
2010 and tree rings, *P. Natl. Acad. Sci. USA*, 109, 5967–5971,
2011 doi:10.1073/pnas.1118965109, 2012.
- 2012 Stine, S.: Extreme and persistent drought in California and Patagonia during medieval
2013 time, *Nature*, 369, 546–549, 1994.
- 2014 Stothers, R. B.: Mystery cloud of AD 536, *Nature*, 307, 344–345,
2015 doi:10.1038/307344a0, 1984.
- 2016 Stuiver, M. and Reimer, P. J.: Extended ¹⁴C data base and revised Calib 3.0 ¹⁴C age
2017 calibration program, *Radiocarbon*, 35, 215–230, 1993.
- 2018 Taricco, C., Ghil, M., Alessio, S., and Vivaldo, G.: Two millennia of climate variability
2019 in the Central Mediterranean, *Clim. Past*, 5, 171–181, doi:10.5194/cp-5-171-2009,
2020 2009.
- 2021 Taricco, C., Vivaldo, G., Alessio, S., Rubinetti, S., and Mancuso, S.: A high-resolution
2022 δ¹⁸O record and Mediterranean climate variability, *Clim. Past*, 11, 509–522,
2023 doi:10.5194/cp-11-509-2015, 2015.
- 2024 Ternois, Y., Sicre, M. A., Boireau, A., Marty, J. C., Miquel, J. C.: Production pattern of
2025 alkenones in the Mediterranean Sea, *Geophys. Res. Lett.*, 23, 3171–3174, 1996.
- 2026 Thornalley, D. J. R., Elderfield, H., and McCave, I. N.: Holocene oscillations in
2027 temperature and salinity of the surface subpolar North Atlantic., *Nature*, 457, 711–
2028 714, doi:10.1038/nature07717, 2009.
- 2029 [Thunell, R.C.: Distribution of Recent Planktonic Foraminifera in Surface Sediments of](#)
2030 [the Mediterranean Sea, *Mar Micropaleontol*, 3, 147-173, 1978.](#)
- 2031 Touchan, R., Xoplaki, E., Funkhouser, G., Luterbacher, J., Hughes, M. K., Erkan, N.,
2032 Akkemik, Ü., and Stephan, J.: Reconstructions of spring/summer precipitation for
2033 the Eastern Mediterranean from tree-ring widths and its connection to large-scale
2034 atmospheric circulation, *Clim. Dynam.*, 25, 75–98, 2005.

2035 Touchan, R., Akkemik, Ü., Hughes, M. K., Erkan, N.: May–June precipitation
 2036 reconstruction of southwestern Anatolia, Turkey during the last 900 years from tree
 2037 rings, *Quaternary Res.*, 68, 196–202, 2007.
 2038 Trouet, V., Esper, J., Graham, N. E., Baker, A., Scourse, J. D., and Frank, D. C.:
 2039 Persistent positive North Atlantic Oscillation mode dominated the Medieval Climate
 2040 Anomaly, *Science*, 324, 78, doi:10.1126/science.1166349, 2009.
 2041 Trouet, V., Scourse, J. D., and Raible, C. C.: North Atlantic storminess and Atlantic
 2042 Meridional Overturning Circulation during the last Millennium: reconciling
 2043 contradictory proxy records of NAO variability, *Global Planet. Change*, 84–85, 48–
 2044 55, doi:10.1016/j.gloplacha.2011.10.003, 2012.
 2045 Tsimplis, M. N. and Baker, F.: Sea level drop in the Mediterranean Sea: an indicator of
 2046 deep water salinity and temperature changes?, *Geophys. Res. Lett.*, 27, 1731–1734,
 2047 2000.
 2048 Tsimplis, M. N. and Josey, S. A.: Forcing of the Mediterranean Sea by atmospheric
 2049 oscillations over the North Atlantic, *Geophys. Res. Lett.*, 28, 803–806, 2001.
 2050 Tsimplis, M. N. and Rixen, M.: Sea level in the Mediterranean Sea: the contribution of
 2051 temperature and salinity changes, *Geophys. Res. Lett.*, 29, 1–4,
 2052 doi:10.1029/2002GL015870, 2002.
 2053 Vallefucio, M., Lirer, F., Ferraro, L., Pelosi, N., Capotondi, L., Sprovieri, M., and
 2054 Incarbona, A.: Climatic variability and anthropogenic signatures in the Gulf of
 2055 Salerno (southern-eastern Tyrrhenian Sea) during the last half millennium, *Rend*
 2056 *Lincei*, 23, 13–23, doi:10.1007/s12210-011-0154-0, 2012.
 2057 van Raden, U. J., Groeneveld, J., Raitzsch, M., and Kucera, M.: Mg/Ca in the
 2058 planktonic foraminifera *Globorotalia inflata* and *Globigerinoides bulloides* from
 2059 Western Mediterranean plankton tow and core top samples, *Mar. Micropaleontol.*,
 2060 78, 101–112, doi:10.1016/j.marmicro.2010.11.002, 2011.
 2061 Vargas-Yáñez, M., Moya, F., García-Martínez, M. C., Tel, E., Zunino, P., Plaza, F.,
 2062 Salat, J., and Pascual, J.: Climate change in the Western Mediterranean Sea 1900–
 2063 2008, *J. Marine Syst.*, 82, 171–176, doi:10.1016/j.jmarsys.2010.04.013, 2010.
 2064 Velasco, J. P. B., Baraza, J., and Canals, M.: La depresión periférica y el lomo
 2065 contourítico de Menorca: evidencias de la actividad de corrientes de fondo al N del
 2066 Talud Balear, *Geogaceta*, 20, 359–362, 1996.
 2067 Versteegh, G. J. M., de Leeuw, J.W., Taricco, C., and Romero, A.: Temperature and
 2068 productivity influences on $U^{K'}_{37}$ and their possible relation to solar forcing of the
 2069 Mediterranean winter, *Geochem. Geophys. Geosy.*, 8, Q09005,
 2070 doi:10.1029/2006GC001543, 2007.
 2071 Villanueva, J., Pelejero, C., and Grimalt, J. O.: Clean-up procedures for the unbiased
 2072 estimation of C_{37} alkenone sea surface temperatures and terrigenous n-alkane inputs
 2073 in paleoceanography, *J. Chromatogr.*, 757, 145–151, 1997.
 2074 Wallace, J. M. and Gutzler, D. S.: Teleconnections in the geopotential height field
 2075 during the Northern Hemisphere winter, *Mon. Weather Rev.*, 109, 784–812, 1981.
 2076 Wassenburg, J. A., Immenhauser, A., Richter, D. K., Niedermayr, A., and Riechelmann,
 2077 S.: Moroccan speleothem and tree ring records suggest a variable positive state of
 2078 the North Atlantic Oscillation during the Medieval Warm Period, *Earth Planet. Sc.*
 2079 *Lett.*, 375, 291–302, doi:10.1016/j.epsl.2013.05.048, 2013.
 2080 Weldeab, S., Siebel, W., Wehausen, R., Emeis, K., Schmiedl, G., and Hemleben, C.:
 2081 Late Pleistocene sedimentation in the western Mediterranean Sea: implications for
 2082 productivity changes and climatic conditions in the catchment areas, *Palaeogeogr.*
 2083 *Palaeocl.*, 190, 121–137, 2003.
 2084 Wright, H. E.: *Global Climates since the Last Glacial Maximum*, Minnesota University

- 2085 Press, Minneapolis, 1994.
- 2086 Yu, J., Elderfield, H., Greaves, M., and Day, J.: Preferential dissolution of benthic
2087 foraminiferal calcite during laboratory reductive cleaning, *Geochem. Geophys.*
2088 *Geosy.*, 8, 6, doi:10.1029/2006GC001571, 2007.
- 2089 Zúñiga, D., García-Orellana, J., Calafat, A., Price, N. B., Adatte, T., Sanchez-Vidal, A.,
2090 Canals, M., Sanchez-Cabeza, J. A., Masqué, P., and Fabres, J.: Late Holocene fine-
2091 grained sediments of the Balearic Abyssal Plain, Western Mediterranean Sea, *Mar.*
2092 *Geol.*, 237, 25–36, 2007.

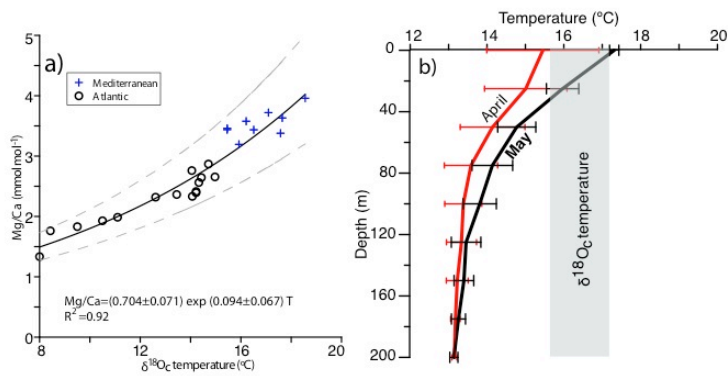
2093
 2094 Table 1. Core tops taken into account in the calibration's adjustment. $\delta^{18}\text{O}_c$ and Mg/Ca
 2095 have been obtained by means of analyses on *G. bulloides* (Mg/Ca procedure have been
 2096 performed without reductive step).
 2097
 2098

<u>Core</u>	<u>Location</u>	<u>Latitude</u>	<u>Longitude</u>	<u>Mg/Ca</u> (mmol mol ⁻¹)	<u>$\delta^{18}\text{O}_c$</u> (VPDB‰)
<u>TR4-157</u>	<u>Balearic Abyssal Plain</u>	<u>40° 30.00' N</u>	<u>4° 55.76' E</u>	<u>3.36</u>	<u>0.53</u>
<u>ALB1</u>	<u>Alboran Sea (WMed)</u>	<u>36° 14.31' N</u>	<u>4° 15.52' W</u>	<u>3.20</u>	<u>0.80</u>
<u>ALBT1</u>	<u>Alboran Sea (WMed)</u>	<u>36° 22.05' N</u>	<u>4° 18.14' W</u>	<u>3.44</u>	<u>0.65</u>
<u>ALBT2</u>	<u>Alboran Sea (EMed)</u>	<u>36° 06.09' N</u>	<u>3° 02.41' W</u>	<u>3.63</u>	<u>0.57</u>
<u>ALBT4</u>	<u>Alboran Sea (EMed)</u>	<u>36° 39.63' N</u>	<u>1° 32.35' W</u>	<u>3.72</u>	<u>0.93</u>
<u>ALBT5</u>	<u>Alboran Sea (EMed)</u>	<u>36° 13.60' N</u>	<u>1° 35.97' W</u>	<u>3.38</u>	<u>0.64</u>



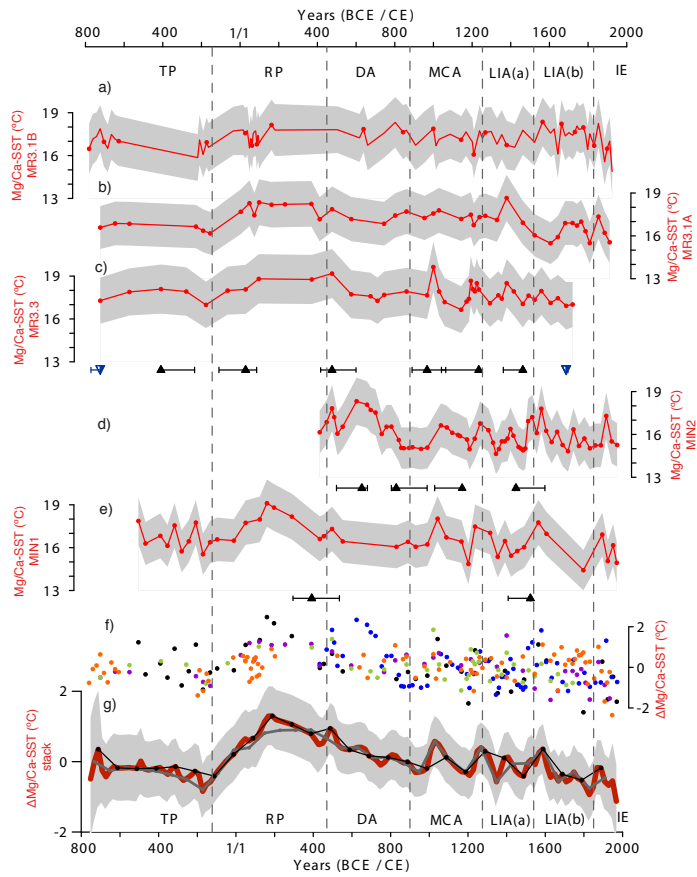
1
2

3 **Figure 1.** Location of the studied area. (a) Central-western Mediterranean Sea: cores MIN
4 and MR3 effect of this study (red dots) with relevant features of surface (NC: Northern
5 Current) and deep water circulation (WMDW: Western Mediterranean Deep Water). (b)
6 Cores used in age-models development from the Tyrrhenian Sea (green triangles) (Lirer et
7 al., 2013) and cores used in Mg/Ca-SST calibration from the Western Mediterranean
8 Basin (blue squares).



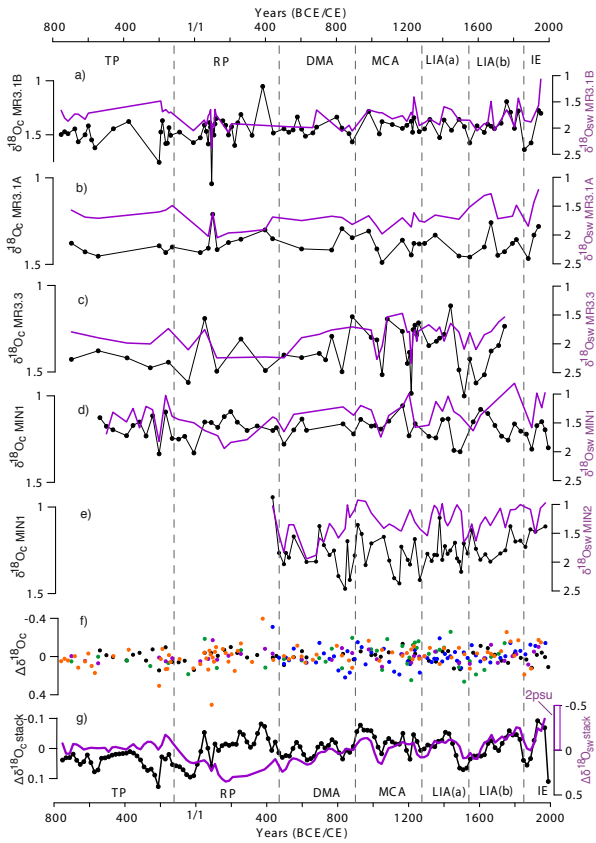
1
2
3
4
5
6
7
8
9
10
11
12

Figure 2. (a) Exponential function and correlation obtained between $\delta^{18}O_c$ temperatures and Mg/Ca for western Mediterranean Sea. Dashed lines show the 1 σ confidence limits of the curve fit. The standard error of our temperature calibration taking into account each $\delta^{18}O_c$ -temperatures from core tops (Table 1) is $\pm 0.6^\circ C$. Error of temperature estimates based on our *G.bulloides* calibration for the Western Mediterranean is $\pm 1.4^\circ C$. These uncertainties are higher but still in the range than $\pm 0.6^\circ C$ obtained for the Atlantic Ocean in Elderfield and Ganssen (2000) and also $1.1^\circ C$ in the same sp. culture data (Lea et al., 1999). (b) April (red) and May (black) temperature profiles of the first 200 m measured during years 1945-2000 in stations corresponding to the studied core tops (MEDAR GROUP, 2002). In grey is shown the $\delta^{18}O_c$ average temperature of all cores.



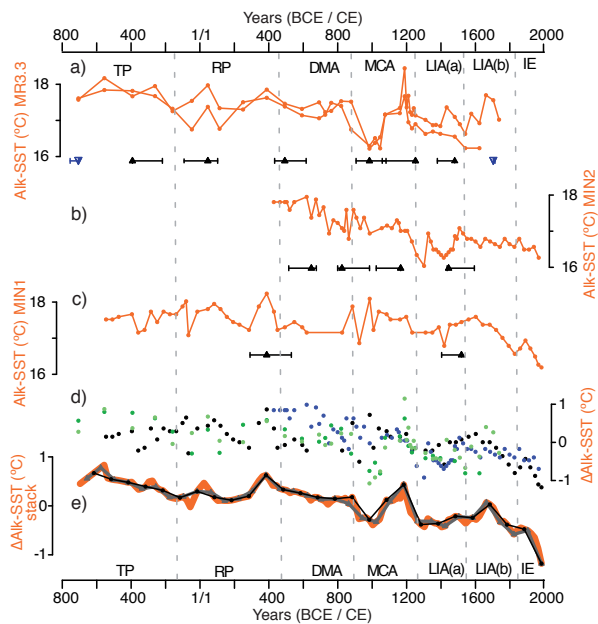
1
2
3
4
5
6
7
8
9
10
11
12
13

Figure 3. SST obtained by means of analysis of Mg/Ca for cores: (a) MR3.1B, (b) MR3.1A, (c) MR3.3, (d) MIN2 and (e) MIN1. Grey-scales integrate uncertainties of average values represent 1σ ; of absolute values include analytical precision and reproducibility and also uncertainties derived *G. bulloides* core top calibrations for the central-western Mediterranean Sea developed in this paper. (f) All individual SST anomalies on their respective time step (MR3.1B: orange, MR3.1A: purple, MR3.3: green, MIN2: blue and MIN1: black dots). (g) 20 yr cm^{-1} stacked temperature anomaly (red plot) with its 2σ uncertainty (grey band). The 80 yr cm^{-1} (grey plot) and the 100 yr cm^{-1} (black plot) stacks are also shown. Triangles represent to ^{14}C dates (black) and biostratigraphical dates based on planktonic foraminifera (blue) and they are shown below the corresponding core and with their associated 2σ errors.

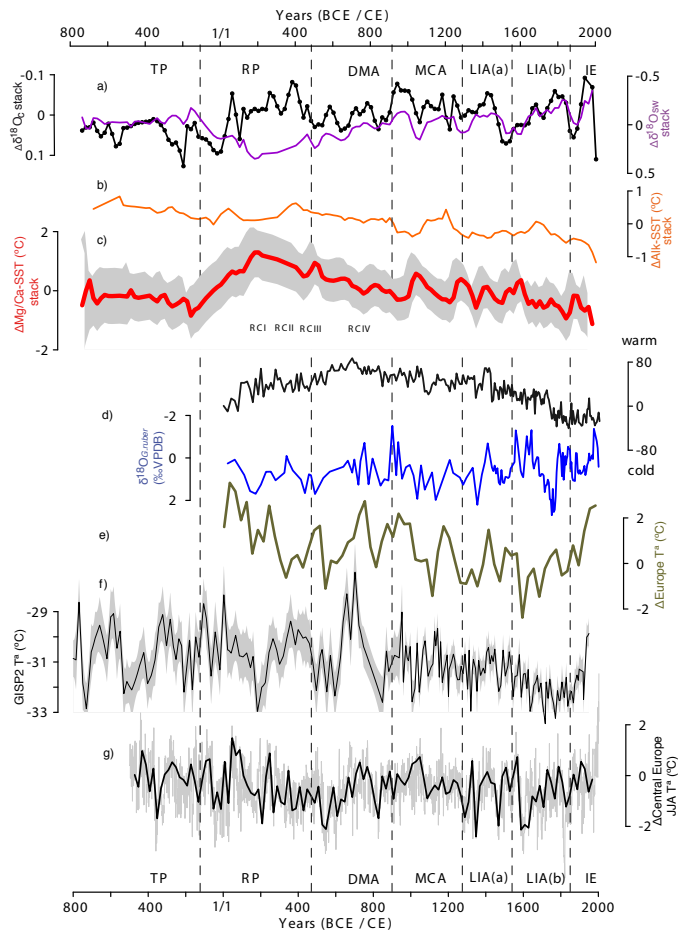


1
2

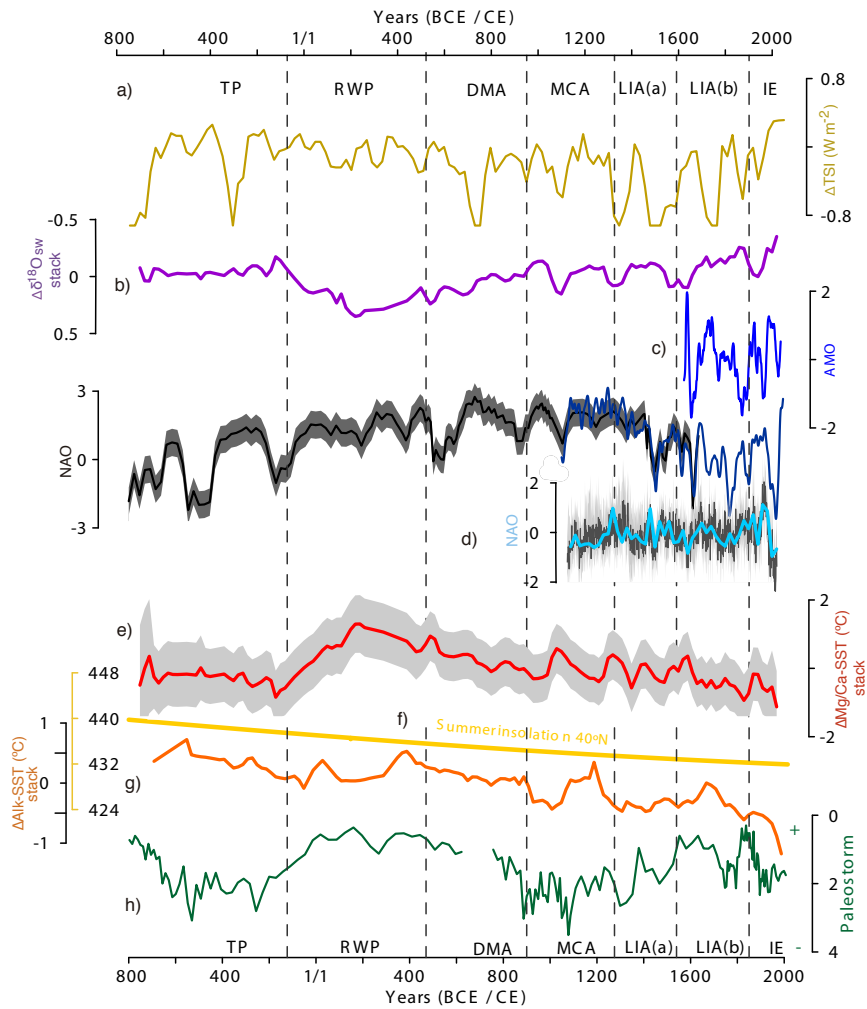
3 | **Figure 4.** Oxygen isotope measured on carbonates shells of *G. bulloides* ($\delta^{18}\text{O}_c$ VPDB‰,
4 | in black) and their derived $\delta^{18}\text{O}_{\text{SW}}$ (purple) for cores: (a) MR3.1B, (b) MR3.1A, (c)
5 | MR3.3 (d) MIN2 and (e) MIN1. (f) Individual $\delta^{18}\text{O}_c$ (VPDB‰) anomalies on their
6 | respective time step. (g) Both respective anomaly stacked records and the equivalence
7 | between $\delta^{18}\text{O}_{\text{SW}}$ (SMOW‰) and salinity, calculated according to Pierre (1999). It is
8 | estimated that the rise of one unit of $\delta^{18}\text{O}_{\text{SW}}$ would amount to an enhancement of 4
9 | practical salinity units.



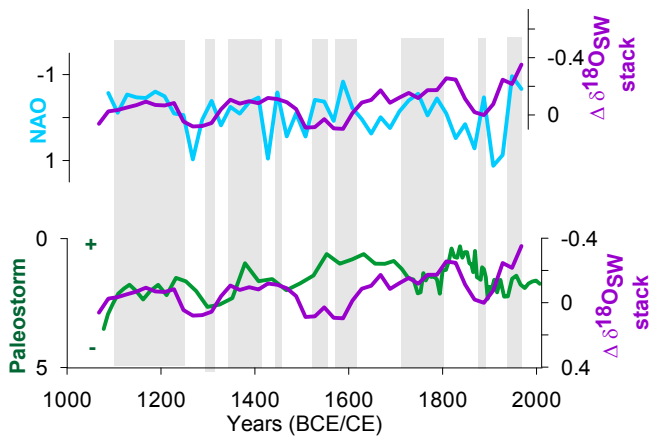
1
2
3 | **Figure 5.** Alkenone temperature records from Minorca (this study) for cores: (a) MR3.3,
4 | (b) MIN2 and (c) MIN1. Triangles represent to ^{14}C dates (black) and biostratigraphical
5 | dates based on planktonic foraminifera (blue) and they are shown below the corresponding
6 | core and with their associated 2σ errors. (d) All individual alkenone derived SST
7 | anomalies on their respective time step (MR3.3: green, MIN2: blue and MIN1: black
8 | dots); (e) 20 yr cm^{-1} stacked temperature anomaly (orange plot). The 80 yr cm^{-1} (**grey** plot)
9 | and the 100 yr cm^{-1} (**black** plot) stacks are also shown.



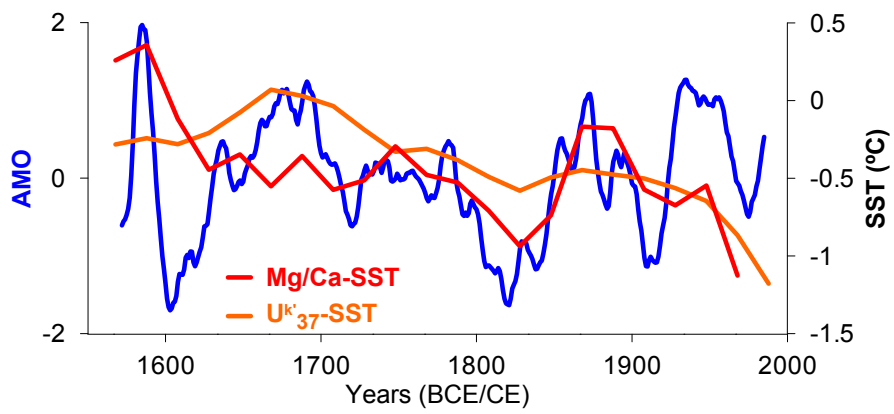
1 |
 2 |
 3 | **Figure 6.** Temperature and isotope anomaly records from Minorca (this study) and data
 4 | from another regions. (a) $\delta^{18}\text{O}_c$ (VPDB‰) and $\delta^{18}\text{O}_{sw}$ (SMOW‰) Minorca stacks, (b)
 5 | Alkenone-SST anomaly Minorca stack, (c) Mg/Ca-SST anomaly Minorca stack, (d) warm
 6 | and cold phases and $\delta^{18}\text{O}_{G.ruber}$ recorded by planktonic foraminifera from the southern
 7 | Tyrrhenian composite core, respectively and RCI to RCIV showing roman cold periods
 8 | (Lirer et al., 2014), (e) 30-year averages of the PAGES 2k Network (2013) Europe
 9 | anomaly Temperature reconstruction, (f) Greenland snow surface temperature (Kobashi et
 10 | al., 2011) and (g) Central Europe Summer anomaly temperature reconstruction in Central
 11 | Europe (Büntgen et al., 2011).



1
 2
 3 **Figure 7.** Temperature and isotope anomaly records from Minorca (this study) and data
 4 from another regions and with external forcings: (a) Total Solar Irradiance (Steinhilber et
 5 al., 2009, 2012), (b) $\delta^{18}\text{O}_{\text{sw}}$ Minorca stacks, (c) Atlantic Multidecadal Oscillation (AMO)
 6 (Gray et al., 2004), (d) North Atlantic Oscillation (NAO) reconstructions (Olsen et al.,
 7 2012, Trouet et al., 2009, and for the last millennium: Ortega et al., 2015), (e) Mg/Ca-SST
 8 anomaly Minorca stack, (f) Summer Insolation at 40 °N (Laskar et al., 2004), g)
 9 Alkenone-SST anomaly Minorca stack and (h) Paleostorm activity in the Gulf of Lions
 10 (Sabatier et al., 2012).



1
 2 | Figure 8. $\delta^{18}\text{O}_{\text{sw}}$ Minorca stack (SMOW‰) during the last millennium (age is expressed
 3 | in years Common Era) plotted with (a) NAO reconstruction (Ortega et al., 2015) and (b)
 4 | Paleostorm activity in the Gulf of Lion (Sabatier et al., 2012). Notice that the NAO axis is
 5 | on descending scale. Grey vertical bars represent negative NAO phases.



1
 2 | Figure 9. Mg/Ca-SST and Alkenone-SST Minorca anomaly stacks during the last
 3 | centuries plotted with AMO reconstruction (Gray et al., 2004).